Euro-Mediterranean Journal for Environmental Integration
https://doi.org/10.1007/s41207-024-00549-5

ORIGINAL PAPER

Natural radioactivity levels and radiation hazards in some magmatic rocks from the eastern and western deserts

M. Abdelmohsen[1] · Mervat A. Elhaddad[2] · Atef El-Taher[1]

Received: 25 December 2023 / Accepted: 11 May 2024

Abstract
This paper reports the natural radioactivity of some igneous rocks used as dimension stones, following the trend of other studies on the evaluation of the risks to human health caused by the rock's natural radioactivity as a consequence of their use as decorative stones and building materials in residential or occupational settings. The whole rock composition of the studied samples was determined using Induced Coupled Plasma Mass Spectrometry ICPMS. Gamma-ray spectrometry has been utilized to determine the ^{40}K, ^{226}Ra, and ^{232}Th activity concentrations in 96 rock types collected from 18 localities. The following activity concentration range was found: 14.88–4148 ^{226}Ra, 4.78–192.08 ^{232}Th, and 206.34–2128.61 ^{40}K Bq/kg. These data were used to measure Ra_{eq}, $H_{ex,}$ and $I\gamma$, besides other parameters, which were compared with the threshold limit values recommended by UNCEAR. They have been exceeded in samples of Qatar, ElDib, and ElGara ElSoda. The results indicated that most of the studied rocks do not present a risk to human health and may be used indoors. The rocks yielded indices above the threshold limit values recommended and could be used outdoors without any restrictions. These findings contribute valuable insight into decision-making processes when using the examined material in the construction of schools, hospitals, museums, factories, and monuments, particularly regarding material safety and radiological risk management.

Keywords Whole rock composition · Natural radionuclides · Activity concentration · Radiological hazards

Introduction

There is no place on earth that is free from radioactivity. Radionuclides such as ^{238}U, ^{232}Th, and ^{40}K emit gamma radiation and their activity concentrations vary from place to place. Soil that contains naturally occurring radionuclides above the maximum permitted exposure limit can be very dangerous and can affect people's health living in that place. This can pose a serious hazard if they are present in high concentrations. Industrial processes such as cement production, mining, oil and gas exploration, and fertilizer production enhance the concentration of the radionuclides (Abbady 2004; Abdul Aziz and Khoo (2018). Consequently, it is crucial to measure the radioactivity levels in rock material to assess their radiological hazards. The knowledge of the amount of natural activity present in rocks used for any application is of prime importance in determining their appropriateness. Public concern led to the engagement of many research teams to measure the natural radioactivity in building materials, underground water, minerals etc. These studies include the works of Abdel Gawad et al. (2023), Taalab et al. (2023), Abed et al. (2022), Awad et al. (2022), Kammar et al. (2022), Agbalagba et al. (2014), Ravisankar et al. (2014), Merle and Enn (2012), Viruthagiri (2011), El-Taher et al. (2010), Prasong and Susaira (2008), Zalewski et al. (2001), among others.

In crystalline rocks, most of the uranium is incorporated into accessory minerals such as monazite, allanite, sphene and zircon so that uranium is not readily accessible for solution and available to secondary mineralization processes (Speer et al. 1981).

The occurrence of naturally occurring radionuclides in construction materials leads to radiation exposure both in outside environments and inner buildings. This is mainly

Responsible Editor: Helder I. Chaminé.

✉ Atef El-Taher
Atef.eltaher@gmail.com

1 Physics Department, Faculty of Science, Al-Azhar University, Assiut, Egypt

2 Geology Department, Faculty of Science, Assiut University, Assiut, Egypt

Published online: 27 June 2024

due to gamma radiation of ^{40}K and members of the U and Th decay series.

Igneous rocks have been extensively used in Egypt as building materials, with granites representing the majority of them. In general, granites are widely recognized to exhibit high levels of U and Th due to the characteristics of the genetic magma and associated tectonic environment.

Rocks generated in the crust are more enriched in radioelements than those formed in the mantle, as a consequence the magma's partial melting and fractional crystallization concentrated them in the liquid phase enhanced in silica.

This paper aims to contribute to a better understanding of the radioactivity of some igneous rocks provided by distinct tectonic environments and commonly used as ornamental or building materials.

General geology

The Eastern Desert of Egypt is a part of the Arabian Nubian Shield. It was classified into three provinces (north, central and south) depending on the variation in lithology and tectonic environments (Stern and Hedge 1985; El Gaby et al. 1988). The border between the NED and CED is demarcated by an intrusive contact, while an extensive shear zone separates the CED from the SED (Stern and Hedge 1985; Fowler et al. 2006). The NED is characterized by ample granitic plutons (syntectonic granitoids) with different gneissic compositions (Windley 1977). This part is devoid of the ophiolitic ultramafics and pillowed tholeiite basalts (Abdel Meguid 1992; El Gaby et al. 1988; El Gaby et al. 1990; Ries et al. 1983; Stern 1981). Lithologically, the CED is composed of larger volumes of ophiolitic sequences and mélanges, ultramafic rocks and pillowed tholeiite basalts, as well as significant portions of arc-type volcanic and volcanogenic sediments (Sims and James 1984). The pre-Pan-African medium-grade gneisses characterized the SED territory. It includes continental shelf facies (meta-sedimentary rocks) which have been intruded by a series of calc-alkaline granitoids (O'Conner et al. 1993).

Most of the southwest of Egypt is a cuesta (small to medium–high escarpment landscape) of Late Jurassic to Cretaceous clastics, with extensive sand and gravel sheets. The Precambrian basement is exposed in some places, covering an area of about 40,000 km2 (Klitzcsh and Schandlemier 1990). The basement separating the deep intra-cratonic Dakhla basin (Egyptian side) from the shallower basins of North Sudan is called "Oweinat- Bir Safsaf- Aswan Uplift", this is the oldest tectonic event "Permo-Triassic" in age (Frantz et al. 1987; Schandlemier and Darbyshire 1984). The uplift is represented by four large enclaves and numerous smaller ones: (1) G. Uweinat (35,000 km^2); (2) Bir Safsaf (2500 km^2). (3) G. El Asr (900 km^2). (4) G. Umm Shaghir (600 km^2).

Geological settings

Our samples were collected from the younger granites of the Eastern and Western Deserts (Figs. 1, 3).The samples covered an area from latitude 27° 52′ 55.00″ N and longitude 33° 0′ 46.90″ E (north Eastern Desert NED) to latitude 24° 35′ 57.80″ N and longitude 34° 9′ 1.60″ E (south the Eastern Desert SED). In the Western Desert, the samples were collected from latitudes 23° 24′ 8.09″ N–23° 11′ 19.00″ N and longitudes 31° 23′ 29.10″ E–31° 49′ 52.20″ E. Accordingly, it is difficult to give detailed geological settings for the eighteen localities where the rock samples were collected. Therefore, only outlines of the geological settings and geochemical characteristics of the granitic samples collected will be presented here.

Granites are widely distributed in the Neoproterozoic rocks of Egypt. They constitute about 60% of its plutonic assemblage (Hussein and ElRamly 1982). The main granitic masses are exposed in the Eastern Desert of Egypt, where the granite plutons intruded into the pre-existing country rocks. Based on their composition, color, and relative age, the granitoid rocks of Egypt are classified into older (750–610 Ma) and younger (620–540 Ma) granites (Akaad and Noweir 1979). They were further classified

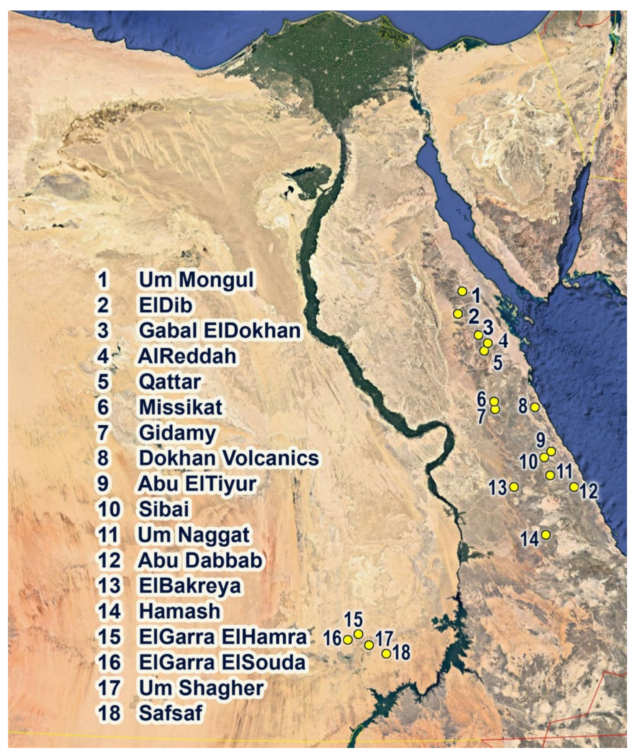

Fig. 1 Google Earth view for the samples' location

(Hussein et al. 1982) to (1) subduction-related older granites; (2) suture-related or post-orogenic younger granites and (3) intraplate anorogenic younger granites. The older granites comprise mainly tonalites and granodiorites, with minor trondhjemite and quartz diorites. According to their geological setting (Akaad et al. 1979), the younger granites are classified into: phase (I) granodiorites with minor monzogranites, phase (II) monzogranites and syenogranites and phase (III) alkali feldspar granites. Recently, Liégeois and Stern (2010) classified the younger granites (phase III). A major tectonic transition for the younger granites was proposed by Stern and Hedge (1985) from a compressive to an extensional regime at 600 Ma. They concluded that the Egyptian granites belong to two main phases of the Pan-African Orogeny: (1) an older group (715–610 Ma) comprises syn- to late-tectonic granites forming batholithic masses with wide compositional variations (trondhjemites to granodiorites with minor granites), and (2) a younger group (600–540 Ma) includes post-tectonic pluton to stock-sized granitic bodies (rich in K-feldspars). Bentor (1985) classified the granites of the Arabian Nubian Shield into two groups: older syn- to late-orogenic granites (880–610 Ma), and younger post-orogenic to orogenic granite (600–475 Ma). Loizenbauer et al. (2001) identified three magmatic pulses in the Central Eastern Desert, dated at 680 Ma; 620 Ma; and 585 Ma.

Topographically, the collected younger granites in this study form high relief. They are intruded with sharp contacts and possess steep walls. They show oval or elongated shapes enclosing mafic xenoliths, enclaves and roof pendants of the country rocks. The granites are pink to red, and medium to coarse-grained (Fig. 1A–D). The younger granites studied are mainly alkali feldspar granite, followed by syenogranite, monzogranite and rare granodiorite. Mineralogically, they are composed of quartz, k-feldspar and plagioclase as essential minerals, with subordinate biotite, muscovite, hornblende (Fig. 2g), riebeckite and arfvedsonite (Fig. e). Allanite, zircon, apatite, sphene, monazite and opaques (iron oxides and pyrite) are the main accessory minerals. Quartz occurs as anhedral large crystals interstitial to other mineral constituents. The potash-feldspars are presented by tabular orthoclase and microcline perthite crystals. Primary K-feldspar minerals are usually altered to sericite and clay minerals (Fig. 2h). The former is corroded by quartz and plagioclase. Plagioclase forms subhedral tabular crystals with albite-lamellar twining to oligoclase composition. In the alkali feldspar granite, quartz is actively intergrown by feldspar leaving blebs of quartz inside the replacing alkali feldspar forming micrographic and myrmekitic textures. Biotite is subordinate (Fig. 2f) and occurs as platy crystals.

Experimental techniques

Samples collection and preparation

A total of 96 fresh samples were collected from eighteen localities in the Eastern and Western Deserts. Forty-eight out of the 96 samples were chemically analyzed, their sampling location is shown in Figs. 1, 3 and Table 1. Samples from the northern part of the Eastern Desert (NED) were gathered the (Gebel G.) G. Um Mongul (Mo), G.ELDib (D), G. El Dokhan (Do), G. Al Reddah (R), and G. Qatar (Q). The samples from the central part covered the areas: G. Missikat (M), G. Gidamy (Gd), El Dokhan Volcanics (Wadi ElQueh) (Dv), G. Abu El Tiyur (At), G. Sibai (Sb), G. Um Naggat (Un), G. Abu Dabbab (Ad), and G. El Bakreya (Bk). The rocks studied from the southern part were assembled from G. Hamash (H). In the Western Desert, the samples were chosen from the southern part where igneous rocks are outcropping: G. El Garra El Hamra (Gh), G. El Garra El Soda (Gs), G. Um Shagher (Us), and around Bir Safsaf (Sf).

For the chemical analysis, the representative collected samples were crushed into a fine powder using a jaw crusher and then sieved to pass a 75 µm mesh screen. All samples were dried at a temperature of 110 °C. For gamma measurement, the samples were sieved by a 200 µm mesh screen. Each sample was weighted and transferred into an airtight cylindrical plastic container (47.6 mm radius, 82 mm height and 0.5 mm thickness). The samples were saved for 4 weeks to attain a secular equilibrium between parents and their short-lived progenies in natural decay chains.

Geochemical analysis

Chemical analysis for the studied rocks was carried out at the commercial laboratories OMAC (Loughrea, Ireland). The major, minor and trace elements were analyzed using Induced Coupled Plasma Mass Spectrometry (ICP-MS). Below the detailed analytical technique is given.

The samples were digested with a concentrated mixture of HNO_3, HF, $HClO_4$ and HCl. The digestion was carried out in two steps. In the first step, the concentrated mixture of HNO_3 (3 mL), HF (2 mL) and $HClO_4$ (0.5 mL) was used. In the second step, the mixture of HNO_3 (3 mL) and HF (1 mL) was added. This is followed by digestion using Aqua Regia (HCl (3 mL): HNO_3 (1 mL) at 200 °C for 2 h in a fume hood. After complete evaporation, the residue was dissolved in 10 mL of 6 M HCl and then dried. The sample solution was prepared in 20 mL of 3% HNO_3. A blank solution was prepared in the same way. An internal

a.Field photos for Um Shagher granite (SWD)

b.Syenite of ElGaraElSoda (SWD)

c. Country rocks in ElGaraElSoda (SWD)

d. Mode of occurrence of granite in Bir Safsaf (SWD)

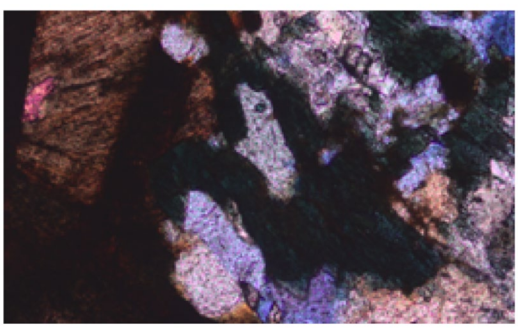

e. Arfvedsonite (black) in ElSibai CN (50µm)

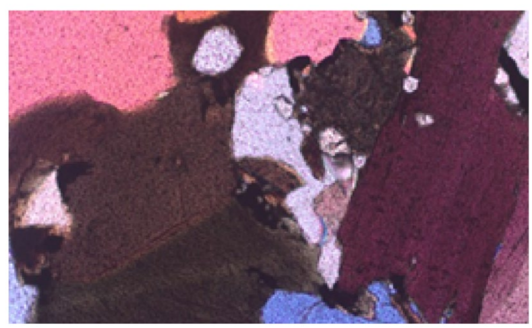

f. Six-sided apatite crystals included in biotite CN (50µm)

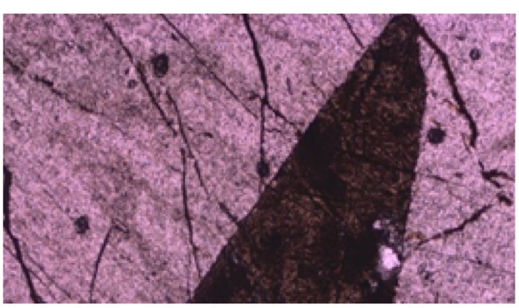

g. Euhedral hornblende in Um ElTiyurPPL(50µm)

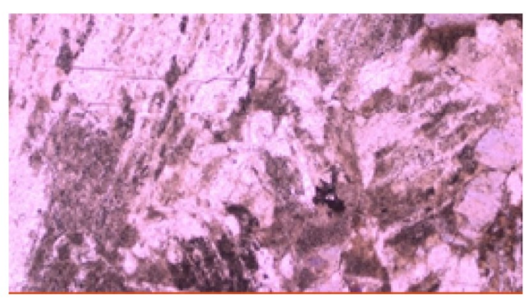

h. Kaolinized feldspar in Qatar PPL (50µm)

Fig. 2 **a**–**d** Field photos and **e**–**h** photomicrographs for some of the studied rocks

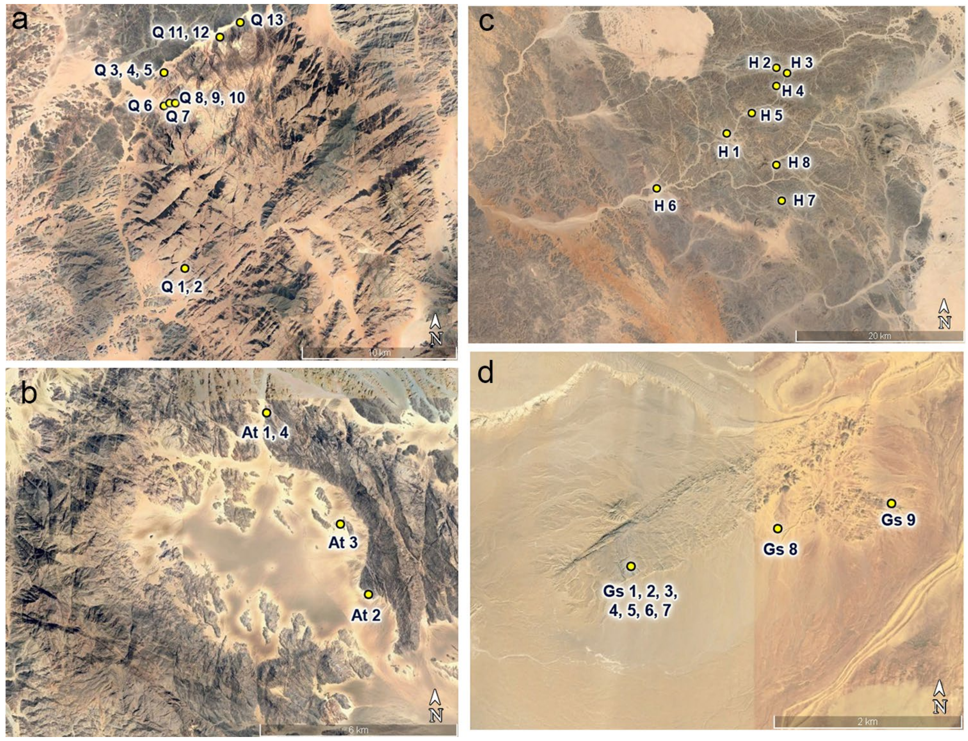

Fig. 3 **a**–**d** Google Earth views for samples' location for Qattar (NED), Abu El Tiyur (CED), Hamash (SED) and ElGara ElSouda (SWD)

standard was spiked into each diluted sample for signal attenuation correction, due to the presence of various elements in the samples as well as for possible changes during ICP-MS measurement. The instrument was operated in a gas mode with He (flowing at 5 mL/min) to remove ion interferences. The ICP-MS detection limit was calculated as three times the standard deviation of the calibration blank measurements ($n = 5$). The detection limits varied from 5 to 0.03 ppm for all elements.

For the gamma-ray spectrometry, each sample was weighted and transferred into an airtight cylindrical plastic container. The samples were saved for 4 weeks towards a secular equilibrium action between parents and their short-lived progenies in natural decay chains.

Gamma ray spectrometer

Measurements of the activity concentrations of ^{238}U, ^{232}Th and ^{40}K in Bq.kg^{-1} for the studied samples were performed using gamma-ray spectrometry. The spectrometer employed for this analysis was a 3 × 3 inch (NaI (Tl) Model 802 with a 2048 multichannel analyzer (MCA). Its assembly were sealed tight, including a high-resolution NaI (Tl) crystal, a photomultiplier tube, an internal magnetic/light shield, an aluminum housing, a 14-pin connector, a preamplifier, a main amplifier, and an analogue-to-digital converter with Genie 2000 software. The detector used had the following specifications: a resolution of 7.5% as specified at the 662 keV peaks of 137Cs, and an aluminum window (thickness 0.5 mm, density 147 mg/cm^3). The oxide reflector (thickness 1.6 mm, density 88 mg/cm^3). The magnetic/light shield is composed of concentric lined steel. The gamma-ray photo peaks corresponded to 1.46 MeV (40 K), 1.76 MeV (214Bi) and 2.614 MeV (208Tl) for the activities of ^{40}K, ^{238}U and^{232}Th, respectively. The sample measuring time (counting spectrum) was approximately in the range between 8 and 24 h. The gamma-ray photopeaks corresponding to 1.4608 MeV (^{40}K) were taken into account to compute ^{40}K activity in the samples. These gamma-ray photopeaks 0.6093, 0.1120, and 1.7645 MeV (^{214}Bi) and 0.2952 and 0.3519 MeV (214Pb) were considered in reaching the ^{238}U activity in the samples. ^{232}Th activity was reached through the gamma-ray photopeaks corresponding to 0.3383, 0.9112 and 0.9689 MeV (^{228}Ac) and 0.5832 and 2.6145 MeV (^{208}Tl) and 0.2386 MeV (^{212}Pb). The detection limit of the detector for ^{40}K, ^{238}U and ^{232}Th was 8.50, 2.21 and 2.11 Bq.kg^{-1}, respectively. The overall uncertainty of the radiation levels was calculated using the propagation law of systematic and random measurement errors. Systematic errors of 0.5–2% existed in the efficiency calibration, and random errors of up to 5% existed in the radioactivity readings (Papadopoulos et al. 2017).

Table 1 The coordinates of the collected samples from the Eastern and Western Deserts

Localities/symbols	Rock type	Sample no.	Plutonic/Volcanic	Latitude (N)	Longitude (E)
G. Um Mongul Mo	Granite	Mo 1	Plutonic	27° 52′ 55″ N	33° 0′ 46.9″ E
	Granite	Mo 2	Plutonic	27° 52′ 55″ N	33° 0′ 46.9″ E
G. EDib D (Frisch and Abdelrahman 1999)	Pegmatitic Syenite	D 1	Plutonic	27° 34′ 23.3″ N	32° 55′ 59.2″ E
	Granite	D 2	Plutonic	27° 34′ 23.3″ N	32° 55′ 59.2″ E
	Granite	D 3	Plutonic	27° 34′ 23.3″ N	32° 55′ 59.2″ E
	Granite	D 4	Plutonic	27° 34′ 23.3″ N	32° 55′ 59.2″ E
	Quartz Syenite	D 5	Plutonic	27° 34′ 23.3″ N	32° 55′ 59.2″ E
	Syenite	D 6	Plutonic	27° 34′ 23.3″ N	32° 55′ 59.2″ E
	Older Trachyte	D 7	Volcanic	27° 34′ 23.3″ N	32° 55′ 59.2″ E
	Younger Trachyte	D 8	Plutonic	27° 34′ 23.3″ N	32° 55′ 59.2″ E
	Older Trachyte	D 9	Volcanic	27° 35′ 11.2″ N	32° 56′ 1.4″ E
	Granite	D 10	Plutonic	27° 34′ 14.8″ N	32° 56′ 7.9″ E
	Younger Trachyte	D 11	Volcanic	27° 34′ 14.8″ N	32° 56′ 7.9″ E
G. Gabal ElDokhan Do (Moghazi 2003)	Granodiorite	Do 1	Plutonic	27° 16′ 50.8″ N	33° 16′ 33.9″ E
	Rhyolite	Do 2	Volcanic	27° 17′ 28.3″ N	33° 17′ 1.9″ E
	Rhyolite	Do 3	Volcanic	27° 18′ 23.5″ N	33° 19′ 27.2″ E
	Biotite Granite	Do 4	Plutonic	27° 18′ 32.2″ N	33° 20′ 9″ E
	Granite	Do 5	Plutonic	27° 18′ 32.2″ N	33° 20′ 9″ E
G. AlReddah R	Granite	R1	Plutonic	27° 10′ 41″ N	33° 20′ 59″ E
Qattar Q (El-Kammar et al. 1997)	Granite	Q 1	Plutonic	27° 6.6′ 31.5″ N	33° 15′ 42.6″ E
	Granite	Q 2	Plutonic	27° 6.6′ 31.5″ N	33° 15′ 42.6″ E
	Quartz Diorite	Q 3	Plutonic	27° 5′ 56.7″ N	33° 14′ 47.2″ E
	Granite	Q 4	Plutonic	27° 5′ 56.7″ N	33° 14′ 47.2″ E
	Granite	Q 5	Plutonic	27° 5′ 56.7″ N	33° 14′ 47.2″ E
	Granite	Q 6	Plutonic	27° 4′ 42.6″ N	33° 14′ 52.7″ E
	Granite	Q 7	Plutonic	27° 4′ 47.3″ N	33° 14′ 57″ E
	Granite	Q 8	Plutonic	27° 4′ 47.3″ N	33° 14′ 57.5″ E
	Granite	Q 9	Plutonic	27° 4′ 47.3″ N	33° 14′ 57.5″ E
	Granite	Q 10	Plutonic	27° 4′ 47.3″ N	33° 14′ 57.5″ E
	Rhyolite	Q 11	Volcanic	27° 7′ 12.2″ N	33° 17′ 6.8″ E
	Granite	Q 12	Plutonic	27° 7′ 12.2″ N	33° 17′ 6.8″ E
	Granite	Q 13	Plutonic	27° 7′ 50.9″ N	33° 17′ 57.9″ E
G. Missikat M Awad (2022)	Granite	M 1	Plutonic	26° 27′ 28.8″ N	33° 24′ 54.9″ E
G. Gidamy Gd El Mezayen (2017)	Rhyolite	Gd 1	Volcanic	26° 26′ 6.2″ N	33° 25′ 15.7″ E

Table 1 (continued)

Localities/symbols	Rock type	Sample no.	Plutonic/Volcanic	Latitude (N)	Longitude (E)
G. Dokhan Volcanics (WadiElQueh) Dv (Ressetar and Monrad 1982)	Latite	Dv 1	Volcanic	26° 6′ 42″ N	34° 10′ 57.6″ E
	Latite	Dv 2	Volcanic	26° 6′ 42″ N	34° 10′ 57.6″ E
	Trachyte	Dv 3	Volcanic	26° 6′ 42″ N	34° 10′ 57.6″ E
	Rhyolite	Dv 4	Volcanic	26° 6′ 22″ N	34° 12′ 14″ E
	Andesite	Dv 5	Volcanic	26° 6′ 22″ N	34° 12′ 14″ E
	Andesite	Dv 6	Volcanic	26° 20′ 14.6″ N	34° 3′ 35″ E
	Andesite	Dv 7	Volcanic	26° 19′48.7″ N	34°2′54.4″ E
	Trachyte	Dv 8	Volcanic	26° 19′48.7″ N	34° 2′54.4″ E
	Trachyte	Dv 9	Volcanic	26° 19′48.7″ N	34° 2′54.4″ E
	Andesite	Dv 10	Volcanic	26° 19′48.7″ N	34° 2′54.4″ E
	Trachy-Andesite	Dv 11	Volcanic	26° 19′ 48.7″ N	34° 2′ 54.4″ E
	Rhyolite	Dv 12	Volcanic	26° 20′ 14.1″ N	34° 4′ 18.4″ E
G. Abu ElTiyur At (Sidique et al. 2021)	Granite	At 1	Plutonic	25° 45′ 42.6″ N	34° 12′ 47.11″ E
	Granite	At 2	Plutonic	25° 42′ 44.1″ N	34° 14′ 42.5″ E
	Granite	At 3	Plutonic	25° 43′ 57.1″ N	34° 14′ 10.8″ E
	Granite	At 4	Plutonic	25° 45′ 42.6″ N	34° 12′ 47.11″ E
Sibai Sb Abdel-Rahman and El-Kibbi (2001)	Granite	Sb 1	Plutonic	25° 41′ 57.8″ N	34° 11′ 56″ E
	Syenite	Sb 2	Plutonic	25° 41′ 57.8″ N	34° 11′ 56″ E
Um Naggat Un (Abdallah et al. 2000)	Granite	Un 1	Plutonic	25° 29′ 02.6″ N	34° 15′ 21.2″ E
	Syenogranite	Un 2	Plutonic	25° 29′ 02.6″ N	34° 15′ 21.2″ E
	Granite	Un 3	Plutonic	25° 29′ 02.6″ N	34° 15′ 21.2″ E
	Granite	Un 4	Plutonic	25° 29′ 17.1″ N	34° 15′ 24.1″ E
	Granite	Un5	Plutonic	25° 28′ 17.8″ N	34° 14′ 20.2″ E
	Granite	Un 6	Plutonic	25° 28′ 17.8″ N	34° 14′ 20.2″ E
	Granite	Un 7	Plutonic	25° 27′ 54.9″ N	34° 14′ 6.5″ E
	Granite	Un 8	Plutonic	25° 27′ 54.9″ N	34° 14′ 6.5″ E
	Granite	Un 9	Plutonic	25° 27′ 31.5″ N	34° 14′ 38.2″ E
	Granite	Un 10	Plutonic	25° 28′ 14.3″ N	34° 15′ 52.5″ E
Abu Dabbab Ad Heikal (2019)	Granite	Ad 1	Plutonic	25° 6′ 12.6″ N	34° 39′ 3.8″ E
	Granite	Ad 2	Plutonic	25° 7′ 32.7″ N	34° 37′ 46″ E
	Granite	Ad 3	Plutonic	25° 18′ 49.7″ N	34° 31′ 57.5″ E
	Syenite	Ad 4	Plutonic	25° 18′ 58.2″ N	34° 31′ 50.2″ E
	Andesite-Basalt	Ad 5	Volcanic	25° 19′ 24.3″ N	34° 37′ 18.5″ E
	Syenite	Ad 6	Plutonic	25° 19′ 48.8″ N	34° 38′ 35.4″ E
ElBakreya Bk (Abd El-Fatah et al. 2023)	Granite	Bk 1	Plutonic	25° 18′ 46.3″ N	33° 42′ 53.1″ E
	Granite	Bk 2	Plutonic	25° 18′ 46.3″ N	33° 42′ 53.1″ E
	Syenite	Bk 3	Plutonic	25° 18′ 46.3″ N	33° 42′ 53.1″ E
	Granite	Bk 4	Plutonic	25° 18′ 21.2″ N	33° 42′ 43.5″ E

Table 1 (continued)

Localities/symbols	Rock type	Sample no.	Plutonic/Volcanic	Latitude (N)	Longitude (E)
Hamash H (Gharib et al. 2021)	Andesite-Basalt	H 1	Volcanic	24° 40′ 9″ N	34° 5′ 8″ E
	Andesite	H 2	Volcanic	24° 44′ 10.7″ N	34° 08′ 40″ E
	Andesite	H 3	Volcanic	24° 44′ 2.4″ N	34° 09′ 8.1″ E
	Basalt	H 4	Volcanic	24° 43′ 24.9″ N	34° 08′ 55.5″ E
	Andesite-Basalt	H 5	Volcanic	24° 41′ 45.9″ N	34° 07′ 1.4″ E
	Basalt	H 6	Volcanic	24° 36′ 41.6″ N	34° 00′ 11.9″ E
	Trachy-Basalt	H 7	Volcanic	24° 35′ 57.8″ N	34° 09′ 1.6″ E
	Trachyte	H 8	Volcanic	24° 38′ 9.4″ N	34° 08′ 31.3″ E
El Garra El Hamra Gh	Quartz Syenite	Gh 1	Plutonic	23° 23′ 38.9″ N	31° 23′ 29.1″ E
	Syenite	Gh 2	Plutonic	23° 23′ 55.1″ N	31° 24′ 1.3″ E
El Garra El Souda Gs	Syenite	Gs 1	Plutonic	23° 21′ 51.0″ N	31° 18′ 38.2″ E
	Syenite	Gs 2	Plutonic	23° 21′ 51.0″ N	31° 18′ 38.2″ E
	Latite	Gs 3	Volcanic	23° 21′ 51.0″ N	31° 18′ 38.2″ E
	Latite	Gs 4	Volcanic	23° 21′ 51.0″ N	31° 18′ 38.2″ E
	Quartz Syenite	Gs 5	Plutonic	23° 21′ 51.0″ N	31° 18′ 38.2″ E
	Syenite	Gs 6	Plutonic	23° 21′ 51.0″ N	31° 18′ 38.2″ E
	Granite	Gs 7	Plutonic	23° 21′ 51.0″ N	31° 18′ 38.2″ E
	Granite	Gs 8	Plutonic	23° 22′ 4.8″ N	31° 19′ 34.3″ E
	Latite	Gs 9	Volcanic	23° 22′ 15.7″ N	31° 20′ 18.8″ E
Um Shagher Us Assran (2015)	Syenite	Us 1	Plutonic	23° 15′ 57.3″ N	31° 28′ 20.3″ E
	Granite	Us 2	Plutonic	23° 16′ 4.1″ N	31° 36′ 21.9″ E
Bir Safsaf Sf (Assran (2015)	Granite	Sf1	Plutonic	23° 11′ 19.0″ N	31° 49′ 52.2″ E
	Granite	Sf2	Plutonic	23° 11′ 19.3″ N	31° 49′ 33.8″ E
	Granite	Sf3	Plutonic	23° 11′ 37.9″ N	31° 49′ 25.4″ E

Analytical method

Activity concentration

The activity concentration (A) of the rock samples, measured in Becquerel per kilogram (Bq.kg^{-1}) was determined using the following equation:

$$A = \frac{Np \times 100}{\eta \times T \times m \times I_{\gamma}} \quad (1)$$

Np represents the peak counts of the sample minus the peak counts of the background (BG), I_γ denotes the emitted gamma ray intensity, T is the counting time, η the measured efficiency for each gamma line, and m the sample mass in kilograms (Uosif and El-Taher 2008).

Radiological hazard

The radium equivalent activity (Ra$_{eq}$)

To assess the radiation hazard associated with the building materials used, the Raeq was estimated, where all the decay products of ^{238}U and ^{232}Th are in radioactive equilibrium with their precursors. Ra$_{eq}$ is calculated according to the formula (EC 1999):

$$Ra_{eq} = A_U + 1.43A_{Th} + 0.0077A_K \quad (2)$$

where A_U, A_{Th}, and A_K speak for the radium equivalent activity of ^{238}U, ^{232}Th, and ^{40}K in Bq.kg^{-1}, respectively.

This formula is based on: 1 $Bq.kg^{-1}$ of ^{238}U, 0.7 $Bq.kg^{-1}$ of ^{232}Th and 13 $Bq.kg^{-1}$ of ^{40}K, producing the same gamma-ray dose rate. This index (Ra_{eq}) is related to both internal (due to the radon) and external gamma doses, it should have the value of 370 $Bq.kg^{-1}$ for the safe use of the building materials.

The absorbed dose rates (D) resulting from gamma radiation in the air at a height of 1 m above the ground surface (UNSCEAR 2000) to fulfil the uniform distribution of the naturally occurring radionuclides ^{238}U, ^{232}Th, and ^{40}K. Conversion factors were applied to compute the absorbed gamma dose rate (D) in air per unit activity concentration in $Bq.kg^{-1}$ which is 0.462 $nGy.h^{-1}$ for ^{238}U, 0.604 $nGy.h^{-1}$ for ^{232}Th, and 0.042 $nGy.h^{-1}$ for ^{40}K. The calculation of D can be carried out using the Eq. (Knežević, et al. 2020).

$$D = 0.462A_U + 0.604A_{Th} + 0.0417A_K \quad (3)$$

where A_U, A_{Th}, and A_K represent the concentration of ^{238}U, ^{232}Th, and ^{40}K in $Bq.kg^{-1}$, respectively.

The world average (UNSCEAR 2000) value of Dis reported as 57 $nGy.h.^{-1}$

The internal hazard index (H_{in}) quantifies the exposure to radon and its daughter products. It is determined from the equation (EC 1999).

$$H_{in} = \frac{A_U}{185} + \frac{A_{Th}}{259} + \frac{A_K}{4810} \quad (4)$$

The External Hazard Index (H_{ex}) assesses exposure to external gamma radiation. It is calculated using the Eq.

$$H_{ex} = \frac{A_U}{370} + \frac{A_{Th}}{259} + \frac{A_K}{4810} \quad (5)$$

where A_U, A_{Th}, A_K represent the concentration of ^{238}U, ^{232}Th, and ^{40}K in $Bq.kg^{-1}$, respectively (Beretka and Matthew 1985).

The Gamma Activity Concentration Index ($I\gamma$) is used to evaluate radiation hazards (European Commission).It is computed according to the Eq.

$$I_\gamma = \frac{A_U}{300} + \frac{A_{Th}}{200} + \frac{A_K}{4000} \quad (6)$$

where A_U, A_{Th}, and A_K stand for the concentration of ^{238}U, ^{232}Th, and ^{40}K in $Bq.kg^{-1}$, respectively. The Iγ value is correlated with the annual dose rate resulting from the excess external gamma radiation caused by surface materials. $I\gamma$ values ≤ 2 correspond to a dose rate criterion of 0.3 $mSv.y^{-1}$, while $I\gamma$ values ≤ 6 correlated with a criterion of 1 $mSv.y^{-1}$. $I\gamma$ should be used as a screening tool to identify materials of concern for construction purposes. Materials with $I\gamma > 6$ should be avoided as it is associated with a dose rate exceeding 1 $mSv.y^{-1}$, which is the maximum recommended for human exposure (El-Taher et al. 2022).

Annual effective dose (AEDE) This parameter examines the conversion coefficient from the absorbed dose in the air to the effective dose and the indoor and outdoor occupancy factors. A conversion coefficient of 0.7 $SvG.y^{-1}$ was utilized for the absorbed dose in air to the effective dose conversion received by adults. The indoor occupancy factor was set at 0.8, to indicate that 20% of the time was spent outdoors and 80% indoors on average worldwide. This parameter is calculated using Eqs. (7) and (8):

$$AEDE_{out}\left(\mu Svy^{-1}\right) = D\left(nGyh^{-1}\right) \times 8760h \times 0.7SvGy^{-1} \times 0.2 \times 10^{-3} \quad (7)$$

$$AEDE_{in}\left(\mu Svy^{-1}\right) = D\left(nGyh^{-1}\right) \times 8760h \times 0.7SvGy^{-1} \times 0.8 \times 10^{-3} \quad (8)$$

where D and AEDE express the absorbed dose rate and annual effective dose, respectively. The World average values (UNCEAR 2000) for indoor and outdoor AEDE are reported as 450 $\mu Sv.y^{-1}$ and 70 $\mu Sv.y^{-1}$, respectively.

Excess lifetime cancer risk (ELCR) This index is computed using the Eq.

$$\text{ELCR} = \text{AEDE} \times \text{DL} \times \text{RF} \quad (9)$$

where AEDE substitutes for the annual effective dose, DL speaks for the duration of life (70 years), and RF serves as the risk factor for fatal cancer risk per Sievert. A value of 0.05 is commonly used (ICRP 1991) by the public to account for the probabilistic effects that occur by chance.

The annual gonadal dose equivalent (AGDE) This parameter results from the specific activities of ^{238}U, ^{232}Th, and ^{40}K. It is computed using Eq. (10)

$$AGDE\left(\mu Sv.y^{-1}\right) = 3.09\,A_U + 4.18\,A_{Th} + 0.314\,A_K \quad (10)$$

where, A_U, A_{Th} and A_K, are the concentrations in ($Bq.kg^{-1}$) for ^{238}U, ^{232}Th and ^{40}K respectively.

Results and discussion

Geochemical characteristics of the studied rocks

The chemical composition of representative samples from the studied localities is given in Table 11. They are highly evolved rocks, judging from the elevated SiO_2 contents. They show an enrichment in Al_2O_3. The rocks' nomenclature was carried out using the TAS plot (NaO_2+KO_2/SiO_2) (Middlemost 1994) (Fig. 4a) as well as the Streckeisen diagram (1979) based on the normative amounts of potash feldspar, quartz and plagioclase. As shown in Fig. 4a that the rocks are mainly granite. The rocks plotted in the diorite and gabbroic diorite fields are actually the volcanic rocks of Dokhan and Hamash. They are andesite and basaltic andesite. The rocks magma is mainly ferroan in composition, while the volcanics plot in the magnesian field (Fig. 4b). The rocks are peraluminous in composition (Fig. 4c). The majority of the rocks plot in the high K calc-alkaline field (Fig. 4d). On the Ga/Al versus Na_2O+KO diagram, the rocks occupied the A-type granites. Some rock samples were plotted within the I-type granites (Dokhan volcanic and Hamashvolcanics) (Fig. 4e). On the tectonic setting diagram, they plot mainly within a plate and few points occupy the volcanic arc field (Fig. 4f).

The activity concentrations of the studied radionuclides

Tables 2, 3, 4, 5 list the results and mean values of the activity concentrations of ^{238}U, ^{232}Th, and ^{40}K for the rock samples collected from the northeastern, central, southeastern and southwestern deserts, respectively.

In the North Eastern Desert, G. Qatar (sample Q10) exhibited the highest activity concentrations of ^{238}U, ^{232}Th, and ^{40}K measured at 4148.79 ± 256.38, 192.08 ± 13.68, and 2314.01 ± 478.67 Bq.kg^{-1}, respectively (Table 2).

Moving to the Central Eastern Desert, the highest activity concentration for ^{232}Th was noted in G. El-Gidamy (sample Gd1) measured at 58.93 ± 5.8779 Bq.kg^{-1}G. Um Naggat, (sample Un7) showed the highest activity concentrations for ^{238}U and ^{40}K, measured at 89.64 ± 8.79 and 1305.07 ± 270.16 Bq.kg^{-1}, respectively (Table 3).

In the Southern Eastern Desert, among the rock samples of G. Hamash, the highest values were recorded in sample (H2) 20.30 ± 2.88, 20.30 ± 2.88 and 266.51 ± 55.25 Bq.kg^{-1} for ^{238}U, ^{232}Th, and ^{40}K, respectively (Table 4).

In the Southern Western Desert, G. El Garra El Souda (sample Gs1) showed the highest activity concentrations for ^{238}U, ^{232}Th, and ^{40}K, noted at 183.52 ± 15.15, 159.95 ± 11.13, and 2128.61 ± 441.54 Bq.kg^{-1}, respectively (Table 5).

In the following, we compare the activity concentrations of ^{238}U, ^{232}Th, and ^{40} K, individually, in the studied rock samples.

The average activity concentrations of ^{238}U (Tables 2, 3, 4, 5) in the North Eastern Desert rocks (NED) measured at Um Mongul, ElDib, G. El Dokhan, El Reddah and Qatar) were 144.86 ± 11.55 Bq.kg^{-1}. The rocks collected at Missikat, Al-Gidamy, Volcanics (Wadi ElQueh), Abu El Tiyur, El Sibai Um Naggat, Abu Dabbab and El Bakreya in the Central Eastern Desert (CED) showed average values of 49.48 ± 5.43 Bq.kg^{-1}. In the Southeastern Desert (SED), the average measured values for Hamash (H) were 12.68 ± 2.59 Bq.kg^{-1}, whereas in the Southwestern Desert (SWD) rocks El Gara El Hamra, El Gara El Soda, Um Shagher and Bir Safsaf measured 69.46 ± 7.08 Bq.kg^{-1}. ^{238}U showed the highest activity concentration in the rocks from the north, southwest, and central-eastern desert and the least activity was in the SED. Thus the rock samples studied from the NED, CED and SWD exceeded the World average value of ^{238}U (35 Bq.kg^{-1}).

^{232}Th average activity concentrations of the rock samples from the North Eastern Desert (NED) was 61.95 ± 5.83 Bq.kg^{-1}, while the rock samples showed an average of 28.49 ± 2.88 Bq.kg^{-1}in the rocks of the Central Eastern Desert (CED). The average values for the rocks Southeastern Desert were 6.93 ± 1.15 Bq.kg^{-1}. Whereas, in the Southwestern Desert (SWD), the average values measured were 58.02 n ± 5.06 Bq.kg^{-1}. The concentration of ^{232}Th in the rocks studied is like that of ^{238}U where they are enriched in the north and impoverished in the southeastern desert. The mean value of ^{232}Th reported in the rocks of the northeastern desert NED (Missikat, Al-Gidamy, Volcanics (Wadi El Queh), Abu El Tiyur, El Sibai Um Naggat, Abu Dabbab and El Bakreya) and southwestern desert SWD El Gara El Hamra, El Gara ElSoda, Um Shagher and Bir Safsaf surpass the value of the World Reference Standard (50 Bq.kg^{-1}) (UNCEAR 2008).

The average activity concentrations of ^{40}K in the rocks of the North Eastern Desert (NED) were 1099.88 ± 227.69 Bq.kg^{-1}, while in the Central Eastern Desert (CED) rocks, the average values were 877.85 ± 182.27 Bq.kg^{-1}. In the Southeastern Desert (SED), the measured values for the rocks showed an average of 108.87 ± 23.48 Bq.kg^{-1}, while in the South Western Desert (SWD), the computed values were 1144.37 ± 237.49 Bq.kg^{-1}. The values of ^{40}K in the rocks under investigation exceeded the Worldwide average (UNCEAR 2008) of ^{40}K (400 Bq.kg^{-1}) except for the volcanic rocks of Hamash in the SED.

Table 6 and Fig. 5 show the results of the natural radioactivity levels of the investigated granites versus the previously studied granites compared to those from Egypt and other countries.

As shown in Table 6, the comparison revealed distinct patterns of radionuclide concentrations among the rocks studied. Specifically, the concentration of ^{238}U exceeded the global average in all regions except in the rocks from SED, due to the enrichment of uranium-rich accessory minerals like monazite, zircon, and xenotime in these rocks. On the other hand, ^{232}Th concentrations are higher than the global

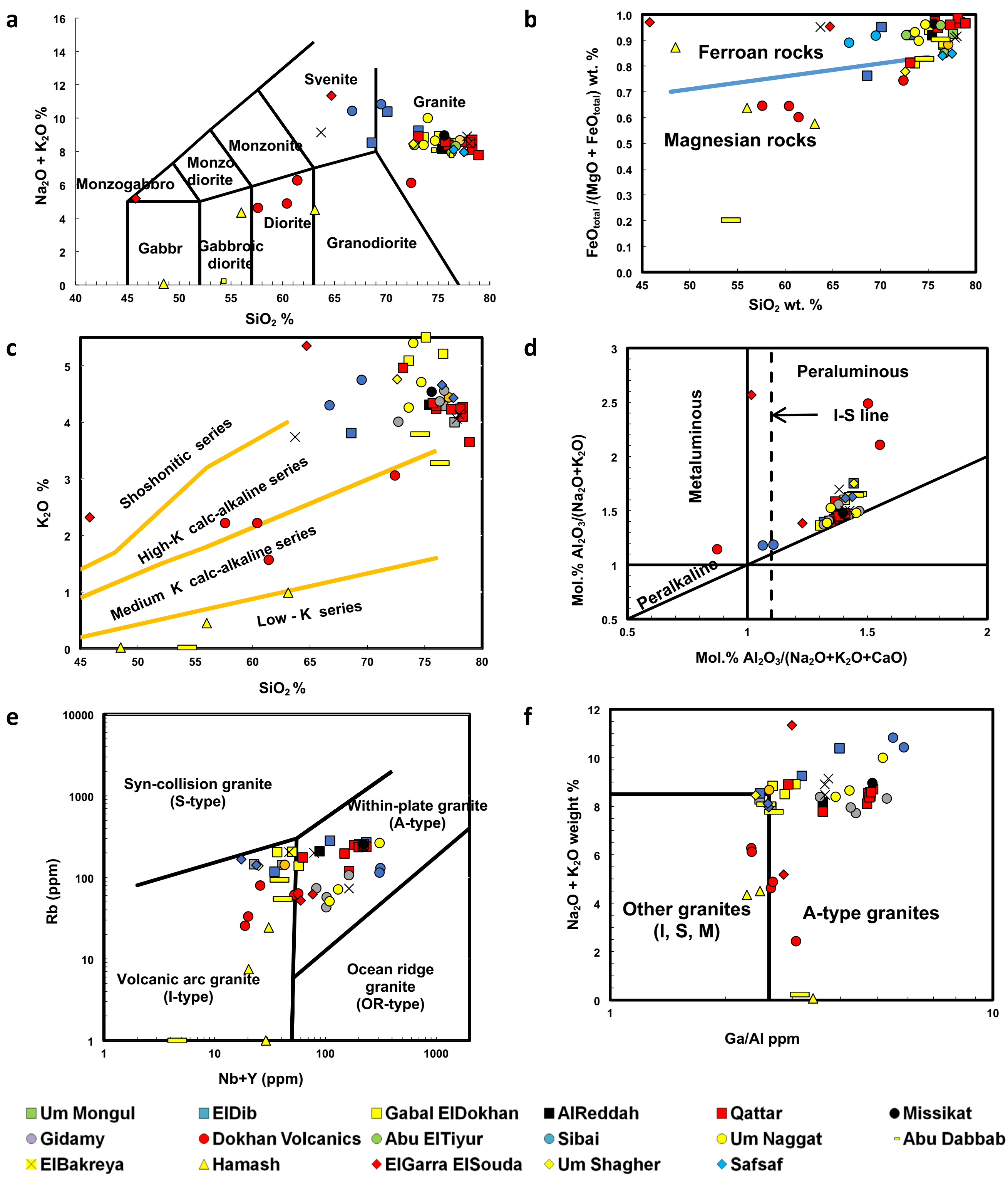

Fig. 4 **a** Classification of the studied rocks (Middlemost 1994) **b** Kind of magma for the studied rocks **c** Variation diagram of K_2O vs. SiO_2 (fields after Rickwood (1989) **d** A/CNK vs. A/NK diagram (Maniar et al. (1989) **e** Tectonic discrimination diagram, Rb versus (Nb + Y) diagram (Pearce 1984). **f** Ga/Al versus $Na_2O + K_2O$ discrimination diagram (Whalen et al. 1987)

Table 2 Activity concentrations of ^{238}U, ^{232}Th and ^{40}K (in $Bq.kg^{-1}$) in the Northeastern desert rock samples

Localities	Samples		Activity concentration in [$Bq.kg^{-1}$]		
	Rock	ID	^{238}U	^{232}Th	^{40}K
G. Um Mongul Mo	Granite	Mo1	77.34 ± 7.47	44.03 ± 4.46	1028.10 ± 212.86
	Granite	Mo2	55.09 ± 6.05	57.55 ± 4.42	961.43 ± 199.06
	Mean		66.21 ± 6.76	50.79 ± 4.44	994.77 ± 205.96
G. EDib D (Frisch and Abdelrahman 1999)	Pegmatitic Syenite	D 1	184.49 ± 17.94	120.80 ± 13.71	1496.98 ± 309.91
	Granite	D 2	63.47 ± 6.45	38.97 ± 4.38	824.81 ± 170.83
	Granite	D 3	69.90 ± 6.60	47.48 ± 4.72	959.46 ± 198.69
	Granite	D 4	55.39 ± 5.26	35.71 ± 3.03	1244.50 ± 257.66
	Quartz Syenite	D 5	39.86 ± 2.94	23.45 ± 2.16	1490.36 ± 308.29
	Syenite	D 6	65.14 ± 6.35	65.12 ± 5.32	1259.70 ± 260.70
	Older Trachyte	D 7	68.01 ± 7.03	67.77 ± 5.41	1287.63 ± 266.54
	Younger Trachyte	D 8	115.02 ± 11.46	124.96 ± 13.97	1262.06 ± 261.29
	Older Trachyte	D 9	73.43 ± 6.65	34.72 ± 3.60	947.79 ± 196.25
	Granite	D 10	69.04 ± 6.89	48.27 ± 4.66	671.20 ± 139.07
	Younger Trachyte	D 11	133.12 ± 12.57	161.17 ± 19.96	1244.78 ± 257.69
	Mean		85.17 ± 8.19	69.86 ± 7.36	1153.57 ± 238.81
G. Gabal ElDokhan Do (Moghazi 2003)	Granodiorite	Do1	70.00 ± 6.68	29.37 ± 2.85	932.48 ± 193.09
	Rhyolite	Do2	68.02 ± 5.88	42.88 ± 4.28	1310.00 ± 271.15
	Rhyolite	Do 3	80.02 ± 7.35	56.28 ± 5.77	1313.19 ± 271.83
	Biotite Granite	Do 4	74.62 ± 7.64	84.09 ± 6.94	1198.16 ± 248.02
	Granite	Do5	76.49 ± 7.83	93.57 ± 8.06	1203.67 ± 249.05
	Mean		73.83 ± 8.19	61.24 ± 7.36	1191.50 ± 238.81
G. AlReddah R	Granite	R1	69.15 ± 6.90	64.39 ± 6.03	1091.40 ± 225.93
	Mean		69.15 ± 6.90	64.39 ± 6.03	1091.40 ± 225.93
Qattar Q (El Kammar et al. 1997)	Granite	Q 1	124.35 ± 10.73	76.86 ± 7.70	1533.18 ± 317.44
	Granite	Q 2	84.03 ± 8.22	44.40 ± 4.27	1037.07 ± 214.72
	Quartz Diorite	Q 3	81.36 ± 6.41	52.24 ± 5.25	1031.49 ± 213.57
	Granite	Q 4	84.29 ± 7.86	48.81 ± 5.27	998.22 ± 206.64
	Granite	Q 5	101.87 ± 9.79	43.12 ± 4.49	1045.58 ± 216.49
	Granite	Q 6	76.49 ± 7.45	72.31 ± 5.76	908.42 ± 188.11
	Granite	Q 7	58.56 ± 5.73	46.43 ± 5.76	990.71 ± 205.13
	Granite	Q 8	435.41 ± 27.09	96.51 ± 6.72	471.04 ± 97.44
	Granite	Q 9	231.98 ± 21.17	32.68 ± 4.35	1126.88 ± 233.35
	Granite	Q 10	4148.79 ± 256.38	192.08 ± 13.68	2314.01 ± 478.67
	Rhyolite	Q 11	48.86 ± 4.80	51.75 ± 4.55	998.43 ± 206.58
	Granite	Q 12	98.44 ± 6.58	63.39 ± 6.26	1081.24 ± 223.85
	Granite	Q 13	14.88 ± 2.23	4.78 ± 0.84	349.73 ± 72.57
	Mean		429.95 ± 28.80	63.49 ± 5.76	1068.15 ± 221.12
Minimum			14.88 ± 2.23	4.78 ± 0.84	349.73 ± 72.57
Maximum			4148.79 ± 256.38	192.08 ± 13.68	2314.01 ± 478.67
Mean			144.86 ± 11.55	61.95 ± 5.83	1099.88 ± 227.69

average in the rocks of the NED and SWD, but lower in the CED and SED rocks, suggesting enrichment of the accessory minerals allanite, and monazite minerals in the rock samples of both parts. Furthermore, ^{40}K concentrations are exceled in all studied parts of both desserts, due to the high concentration of potash feldspars in rocks.

Radiological hazard parameters

The activity concentrations of naturally occurring radionuclides in building materials have been reported in several publications, which can vary according to the type and origin of the building material.

Table 3 Activity concentrations of ^{238}U, ^{232}Th and ^{40}K (in Bq.kg^{-1}) in the rock samples from the Central Eastern Desert

Localities	Samples		Activity concentration in [Bq.kg^{-1}]		
	Rock type	ID	^{238}U	^{232}Th	^{40}K
G. Missikat M Awad (2022)	Granite	M 1	64.46 ± 6.24	28.35 ± 3.00	1027.30 ± 212.69
	Mean		64.46 ± 6.24	28.35 ± 3.00	1027.30 ± 212.69
G. Gidamy Gd El Mezayen (2017)	Rhyolite	Gd 1	80.99 ± 7.81	58.93 ± 5.87	988.23 ± 204.63
	Mean		80.99 ± 7.81	58.93 ± 5.87	988.23 ± 204.63
G. DokhanVolcanics (WadiElQueh) Dv (Ressetar and Monrad 1982)	Latite	Dv 1	17.61 ± 3.67	3.22 ± 0.70	361.03 ± 74.87
	Latite	Dv 2	8.89 ± 4.34	6.73 ± 2.94	319.01 ± 66.21
	Trachyte	Dv 3	2.78 ± 0.15	8.76 ± 1.67	119.24 ± 32.52
	Rhyolite	Dv 4	24.37 ± 3.35	10.97 ± 1.38	752.12 ± 155.79
	Andesite	Dv 5	1.28 ± 1.85	1.28 ± 0.52	65.55 ± 14.89
	Andesite	Dv 6	21.98 ± 4.02	7.05 ± 4.97	560.67 ± 116.20
	Andesite	Dv 7	32.14 ± 3.51	13.01 ± 1.30	579.19 ± 120.03
	Trachyte	Dv 8	8.86 ± 3.79	2.39 ± 1.87	26.28 ± 5.62
	Trachyte	Dv 9	8.00 ± 5.63	0.12 ± 0.69	63.48 ± 13.36
	Andesite	Dv 10	20.55 ± 2.10	20.46 ± 2.05	550.86 ± 114.20
	Trachy-Andesite	Dv 11	22.71 ± 3.07	14.01 ± 1.83	794.30 ± 164.50
	Rhyolite	Dv 12	13.89 ± 1.86	11.90 ± 1.60	306.85 ± 63.69
	Mean		15.26 ± 3.11	8.23 ± 1.79	374.88 ± 78.49
G. Abu ElTiyur At (Sidique et al. 2021)	Granite	At 1	41.76 ± 4.04	28.74 ± 1.78	971.27 ± 201.08
	Granite	At 2	29.64 ± 2.51	11.67 ± 1.57	887.63 ± 183.66
	Granite	At 3	26.56 ± 2.40	18.71 ± 1.50	933.37 ± 193.24
	Granite	At 4	38.53 ± 4.18	17.90 ± 1.74	959.65 ± 198.70
	Mean		34.12 ± 3.28	19.25 ± 1.65	937.98 ± 194.17
Sibai Sb (Abdel-Rahman and El-Kibbi 2001)	Granite	Sb 1	74.30 ± 7.10	54.31 ± 5.28	1129.10 ± 233.69
	Syenite	Sb 2	71.46 ± 7.31	52.41 ± 5.03	972.82 ± 201.42
	Mean		72.88 ± 7.20	53.36 ± 5.15	1050.96 ± 217.56
Um Naggat Un (Abdallah et al. 2000)	Granite	Un 1	26.80 ± 2.57	12.89 ± 1.64	1041.28 ± 215.54
	Syenogranite	Un 2	42.22 ± 4.39	25.74 ± 2.52	1047.47 ± 216.87
	Granite	Un 3	36.29 ± 3.21	26.03 ± 2.41	1093.04 ± 226.28
	Granite	Un 4	42.59 ± 3.85	28.71 ± 2.19	1101.94 ± 228.12
	Granite	Un 5	70.14 ± 5.27	39.39 ± 3.39	1029.70 ± 213.17
	Granite	Un 6	44.23 ± 4.71	26.29 ± 1.75	1008.17 ± 208.74
	Granite	Un 7	89.64 ± 8.79	21.49 ± 1.67	1305.07 ± 270.16
	Granite	Un 8	22.97 ± 2.19	23.97 ± 2.51	1043.10 ± 215.94
	Granite	Un 9	25.51 ± 1.68	15.55 ± 1.64	1127.96 ± 233.38
	Granite	Un 10	66.48 ± 6.76	40.63 ± 3.74	880.21 ± 182.27
	Mean		46.69 ± 4.34	26.00 ± 2.35	1067.79 ± 221.05
Abu Dabbab Ad Heikal (2019)	Granite	Ad 1	22.43 ± 2.65	7.56 ± 1.54	802.43 ± 166.16
	Granite	Ad 2	9.42 ± 3.88	1.42 ± 0.28	148.41 ± 30.92
	Granite	Ad 3	26.48 ± 2.45	25.61 ± 2.57	862.38 ± 178.52
	Syenite	Ad 4	22.19 ± 2.38	5.34 ± 0.95	761.08 ± 157.60
	Andesite-Basalt	Ad 5	69.69 ± 19.29	0.02 ± 0.00	92.82 ± 39.20
	Syenite	Ad 6	18.93 ± 7.71	5.20 ± 3.26	843.25 ± 174.59
	Mean		28.19 ± 6.39	7.52 ± 1.44	585.06 ± 124.50
El Bakreya Bk (Abd El-Fatah et al. 2023)	Granite	Bk 1	71.68 ± 6.48	32.83 ± 2.41	997.84 ± 206.41
	Granite	Bk 2	46.73 ± 4.68	29.82 ± 1.70	962.71 ± 199.35
	Syenite	Bk 3	54.79 ± 5.10	25.21 ± 2.76	960.41 ± 198.88
	Granite	Bk 4	39.85 ± 3.97	16.81 ± 1.50	1041.27 ± 215.57
	Mean		53.26 ± 5.06	26.17 ± 2.09	990.56 ± 205.05

Table 3 (continued)

Localities	Samples		Activity concentration in [Bq.kg^{-1}]		
	Rock type	ID	^{238}U	^{232}Th	^{40}K
Minimum			1.28 ± 1.85	0.02 ± 0.001	26.28 ± 5.62
Maximum			89.64 ± 8.79	58.93 ± 5.87	1305.07 ± 270.16
Mean			49.48 ± 5.43	28.49 ± 2.88	877.85 ± 182.27

Table 4 Activity concentrations of ^{238}U, ^{232}Th and ^{40}K (in Bq.kg^{-1}) in the rock samples from the Southeastern Desert

Localities	Samples		Activity concentration in [Bq.kg^{-1}]		
	Rock type	ID	^{238}U	^{232}Th	^{40}K
Hamash H (Gharib et al. 2021)	Andesite-Basalt	H 1	15.59 ± 3.40	8.84 ± 0.55	24.49 ± 11.43
	Andesite	H 2	20.30 ± 2.88	12.81 ± 1.44	266.51 ± 55.25
	Andesite	H 3	9.12 ± 2.33	4.60 ± 3.55	213.94 ± 44.48
	Basalt	H 4	16.47 ± 2.33	9.11 ± 1.21	39.81 ± 8.48
	Andesite-Basalt	H 5	17.35 ± 2.63	9.81 ± 0.82	214.06 ± 44.53
	Basalt	H 6	1.95 ± 2.26	0.08 ± 0.22	0.20 ± 0.16
	Trachy-Basalt	H 7	6.87 ± 2.99	1.67 ± 0.34	0.11 ± 0.16
	Trachyte	H 8	13.82 ± 1.89	8.53 ± 1.06	111.82 ± 23.37
	Average		12.68 ± 2.59	6.93 ± 1.15	108.87 ± 23.48
Minimum			1.95 ± 2.26	0.08 ± 0.22	0.20 ± 0.16
Maximum			20.30 ± 2.88	12.81 ± 1.44	266.51 ± 55.25
Average			12.68 ± 2.59	6.93 ± 1.15	108.87 ± 23.48

Table 5 Activity concentrations of ^{238}U, ^{232}Th and ^{40}K (in Bq.kg^{-1}) in the rock samples from the Southwestern Desert

Localities	Samples		Activity concentration in [Bq.kg^{-1}]		
	Rock type	ID	^{238}U	^{232}Th	^{40}K
El Garra El Hamra Gh	Quartz Syenite	Gh1	55.30 ± 5.25	49.20 ± 4.04	1211.17 ± 250.73
	Syenite	Gh2	43.51 ± 4.29	14.89 ± 2.12	977.52 ± 202.38
	Mean		49.40 ± 4.77	32.05 ± 3.08	1094.35 ± 226.56
El Garra El Souda Gs	Syenite	Gs 1	183.52 ± 15.15	159.95 ± 11.13	2128.61 ± 441.54
	Syenite	Gs2	74.03 ± 5.61	29.92 ± 2.71	1299.88 ± 269.04
	Latite	Gs3	92.86 ± 10.29	114.98 ± 8.00	1102.64 ± 228.30
	Latite	Gs4	13.09 ± 3.50	7.52 ± 3.42	528.32 ± 109.35
	Quartz Syenite	Gs 5	38.01 ± 3.93	14.63 ± 1.31	1379.31 ± 285.54
	Syenite	Gs 6	87.82 ± 8.59	87.83 ± 5.79	1342.00 ± 277.84
	Granite	Gs7	52.96 ± 4.78	28.74 ± 5.85	1351.85 ± 279.82
	Granite	Gs 8	50.95 ± 5.33	44.91 ± 2.85	1173.72 ± 242.98
	Latite	Gs9	4.73 ± 9.96	0.71 ± 1.22	206.34 ± 50.86
	Mean		66.44 ± 7.46	54.35 ± 4.70	1168.07 ± 242.81
Um Shagher Us Assran (2015)	Syenite	Us1	79.93 ± 8.36	83.98 ± 5.92	1276.04 ± 264.19
	Granite	Us2	81.13 ± 7.83	87.86 ± 7.49	1149.72 ± 238.01
	Mean		80.53 ± 8.09	85.92 ± 6.70	1212.88 ± 251.10
Bir Sa (fsaf Sf (Assran (2015)	Granite	Sf1	87.89 ± 8.86	75.96 ± 6.11	1080.88 ± 227.78
	Granite	Sf2	86.63 ± 8.35	50.24 ± 5.59	1020.87 ± 211.35
	Granite	Sf3	69.82 ± 6.73	53.07 ± 5.52	1204.77 ± 249.39
	Average		81.45 ± 7.98	59.76 ± 5.74	1102.17 ± 229.51
Minimum			4.73 ± 9.96	0.71 ± 1.22	206.34 ± 50.86
Maximum			183.52 ± 15.15	159.95 ± 11.13	2128.61 ± 441.54
Average			69.46 ± 7.08	58.02 ± 5.06	1144.37 ± 237.49

Table 6 The average activity concentrations of the investigated rock samples from the Eastern and Southern deserts compared with other countries and world average values

Country/region	Activity ($Bq.Kg^{-1}$)			References
	^{238}U	^{232}Th	^{40}K	
Egypt North Eastern Desert (NED)	145	62	1100	Present work
Central Eastern Desert (CED)	49	28	878	Present work
South Eastern Desert (SED)	13	7	109	Present work
South Western Desert (SWD)	69	58	1144	Present work
Saudi Arabia (Granitic Rocks)	319	487	726	Fathallah and Khattab (2023)
South Eastern Desert of Egypt	610	110	1157	Adel et al. (2022)
Saudi Arabia (Igneous and Sedimentary Rocks)	11	12	1172	Al-Zahrani et al. (2020)
Nigeria (Granites)	43	18	571	Orosun et al. (2019)
Turkey (Granites)	264	207	2542	Papadopoulos et al. (2017)
Egypt (Commercial Granites)	138	82	1081	Amin (2012)
Italy (Commercial Ornamental Stones)	112	107	1063	Marocch et al. (2011)
United States (Commercial Granites)	31	61	1210	Kitto et al. (2009)
Greece (granites used as building materials)	64	81	1104	Pavlidou et al. (2006)
Brazil (commercial granites)	31	73	1648	Anjos et al. (2005)
Cyprus (imported granites)	77	143	1215	Tzortzis et al. (2003)
Egypt (Altered Dokhan Volcanics)	2161	495	1086	Kammar et al. (2022)*
Worldwide	35	50	400	UNSCEAR (2000)

*Kamar MS, Salem IA, El-Aassy IE, El-Sayed AA, Zakaly HM, Alzahrani AM, Lasheen ESR (2022) An Investigation of High-Level Natural Radioactivity and Geochemistry of Neoproterozoic Dokhan Volcanics: A Case Study of Wadi Gebeiy, Southwestern Sinai, Egypt. Sustainability 2022, 14, 9291. https://doi.org/10.3390/su14159291

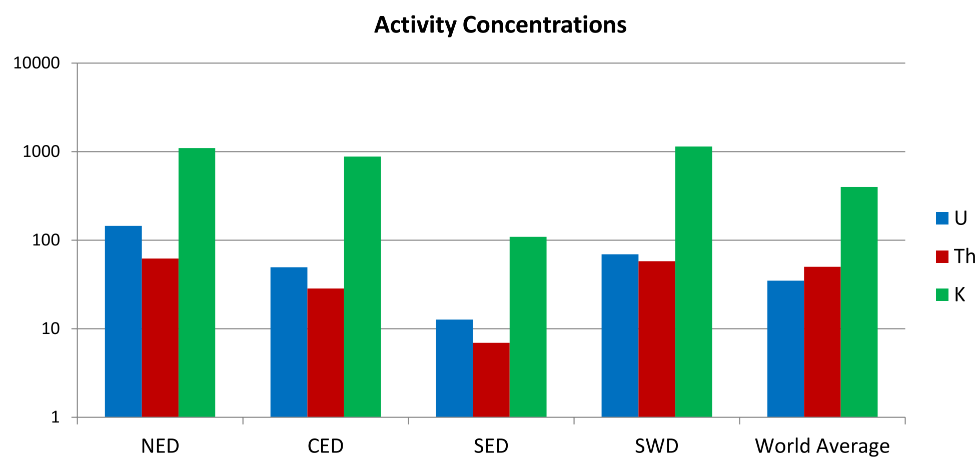

Fig. 5 Comparison between the mean activity concentrations of the studied radioisotopes from the rocks from the four parts of both Deserts compared with the World average

Tables 7, 8, 9, and 10 exhibit the radiation hazards associated with the rock samples collected from the North, Central, Southeastern, and Southwestern Deserts. The calculation intends to provide a comprehensive assessment of the potential radiation risks posed by the investigated rocks.

The radium equivalent (Ra_{eq}) values for the samples under consideration were carefully examined following the recommended safety limit of 370 $Bq.kg^{-1}$ (UNSCEAR 2000). The majority of the samples demonstrated activity Ra_{eq} values below the safety threshold, indicating an acceptable level of radiation. However, several exceptions were observed, as the samples from G. El Dib (D1, D8, and D11) were estimated at 472.50, 390.88 and 459.44 $Bq.kg^{-1}$) and G. Qatar (Q8 and Q10) (609.69 and 4601.65 $Bq.kg^{-1}$) from the Northeastern Desert exceeding the safe limit. In contrast, the rock samples studied from the Central and Southeastern Desert did not surpass the limit. The rocks of G. El Garra El Souda (sample Gs1) (576.16 $Bq.kg^{-1}$) in the Southwestern Desert showed an elevated activity of Ra_{eq} which is attributed to the higher concentrations of ^{238}U in rocks.

The *absorbed dose rates (D)* $nGy \cdot h^{-1}$. It is important to note that the mean D values for all measured rocks exceeded the global average soil value of 59 $nGy \cdot h^{-1}$ reported by UNSCEAR (2000), except those of Dokhan volcanics (Wadi

El Queh) and G. Abu Dabbab (27.40 and 41.51 $nGy \cdot h^{-1}$) in the Central Eastern Desert, as well as the rocks of G. Hamash (14.51 $nGy \cdot h^{-1}$) in the Southeastern Desert. This indicates a significant radiological risk associated with these particular types of rocks.

The *Outdoor Annual Effective Dose Equivalent ($AEDE_{out}$)* ($\mu Sv \cdot y^{-1}$). All the examined rocks surpassed the World average value of outdoor AEDE (70 $\mu Sv \cdot y^{-1}$) reported by UNSCEAR (2000). Except those rocks of Dokhan Volcanics (Wadi ElQueh) and G. Abu Dabbab (33.63 and 50.94 $\mu Sv \cdot y^{-1}$) in the Central East Desert, as well as the volcanics of G. Hamash (17.81 $\mu Sv \cdot y^{-1}$) in the Southeastern Desert.

Concerning the *indoor annual effective dose equivalent* ($AEDE_{in}$) ($\mu Sv \cdot y^{-1}$). This parameter showed that many samples in different localities in the Northeastern Desert and Southwestern Deserts manifested higher AEDE values compared to the World average value of indoor AEDE (450 $\mu Sv \cdot y^{-1}$), except for the rocks of G. El Gara El Hamra (427.33$\mu Sv \cdot y^{-1}$) in the Southwestern Desert. Conversely, in the Central and Southeastern Desert, all localities displayed values lower than the World average, except G. El-Gidamy and G. El Sibai (557.31 and 535.03 $\mu Sv \cdot y^{-1}$) respectively, in the Central Eastern Desert.

The excess lifetime cancer risks (ELCR) utilized the calculated annual effective dose equivalent (AEDE) results for the estimation of the risk associated with the studied rock samples. Remarkably, the mean ELCR values for most examined rocks exceeded the World average value of outdoor ELCR (1450) (Qureshi et al. 2014) except Dokhan volcanics (Wadi ElQueh), G. Abu Dabbab and G. Abu Eltiyur (588.46, 891.44 and 1414.28 $\mu Sv \cdot y^{-1}$) in the Central Eastern Desert, as well as the rock samples from G. Hamash (311.61 $\mu Sv \cdot y^{-1}$) in the Southeastern Desert.

Internal and External Hazard Indices (H_{in}) (H_{ex}). The average values for the studied rocks (Tables 7, 8, 9, 10) were below unity, which is the recommended safe limit. However, the rocks of G. Qatar exhibited mean H_{in} and H_{ex} values of 2.79 and 1.63, respectively, indicating a higher level of internal and external radiological hazards.

Moreover, the $I\gamma$ values for the rock samples under investigation are found to be less than 2, suggesting that the gamma dose originating from these rocks does not exceed 0.3 $mSv \cdot y^{-1}$.

Annual gonadal dose equivalent (AGDE) ($mSv \cdot y^{-1}$) mean values exceeded the Global average soil value of 0.3 $mSv \cdot y^{-1}$ (Xinwei et al. 2006), except for the Dokhan Volcanics (Wadi El Queh) (0.20) in the Central Eastern Desert and the volcanics of G. Hamash (0.10) in the Southeastern Desert (Tables 11, 12).

The contribution of ^{238}U, ^{232}Th and ^{40}K in the studied rock samples

Figures 6a–d illustrate the average contribution of ^{238}U, ^{232}Th, and ^{40}K for the rock samples from the North, Central, Southeastern, and Southwestern Deserts, respectively. The analysis revealed that the input of ^{238}U, ^{232}Th, and ^{40}K were 7.65%, 4.81%, and 87.54%, respectively in the rock samples from the Northeastern Desert. In comparison, they supplied 5.90%, 2.82%, and 91.28%, respectively to the rock samples from the Central Eastern Desert. For the Southeastern Desert, the additions were 31.54%, 8.95%, and 59.51% respectively and for the Southwestern Desert 5.29%, 4.29%, and 90.42%, respectively. As shown in (Fig. 6) that the highest contribution originated from ^{40}K. This isotope occurs in the potash feldspars in all studied rocks, followed by ^{238}U (Fig. 6c), *which* is the most common *isotope* of uranium *found* in nature, with a relative abundance of 99%. Zircon mineral ($ZrSiO_4$) contains ppb amounts of ^{235}U and ^{238}U. This accessory mineral is the most predominant one in all igneous rocks, especially granitic rocks. The contribution of ^{232}Th (Fig. 6) was relatively small due to the relative depletion of the accessory minerals bearing thorium in the studied rock samples.

Pearson correlation between the natural radionuclides

Pearson correlation for the natural radionuclides (^{238}U, ^{232}Th, and ^{40}K) are illustrated in Figures A, B, C, and D for the rocks under investigation. These correlations were performed to determine the interrelation between the natural radionuclides and the calculated radiological hazard parameters (Fig. 7).

The correlation coefficients between (U, Th), (U, K), and (Th, K) were found to be 0.622, 0.628, and 0.589 in the rocks from the North Eastern Desert (NED), while they calculated 0.761, 0.610, and 0.663 in the Central Eastern Desert (CED) samples. The correlations between the radioactive elements in the samples of the Southeastern Desert (SED) were 0.988, 0.558, and 0.600 and 0.918, 0.817, and 0.677 in the Southwestern Desert (SWD) samples, respectively. It is reported (Bashir et al. 2019) that ^{238}U and ^{232}Th are usually found together in nature, and a good correlation between them is indicative of common sources, i.e. associated in the same mineralogical phase. ^{238}U and ^{232}Th are positively correlated with all calculated radiological parameters. This is due to the enrichment of $^{238}U$and ^{232}Th, as both play important roles in determining the hazards associated with the

Table 7 Radiological hazard parameters of the Northeastern Desert rock samples

Localities	Samples		Ra_{eq}	D	AEDE out	AEDE in	H ex	H in	(Iγ)	(I)	(ELCR)	AGDE
	Rock type	ID	$Bq.Kg^{-1}$	$nGy.h^{-1}$	$\mu Sv.y^{-1}$	$\mu Sv.y^{-1}$						$mSv.y^{-1}$
G. Um Mongul Mo	Granite	Mo 1	219.46	104.47	128.22	512.86	0.59	0.80	0.73	1.33	2243.77	0.75
	Granite	Mo 2	211.41	99.63	122.27	489.07	0.57	0.72	0.71	1.28	2139.70	0.71
	Mean		215.44	102.05	125.24	500.97	0.58	0.76	0.72	1.31	2191.74	0.73
G. EDib D (Frisch and Abdelrahman 1999)	Pegmatitic Syenite	D 1	472.50	219.57	269.47	1077.87	1.28	1.77	1.59	3.29	4715.70	1.55
	Granite	D 2	182.70	86.68	106.37	425.49	0.49	0.67	0.61	1.13	1861.54	0.62
	Granite	D 3	211.68	100.31	123.11	492.43	0.57	0.76	0.71	1.30	2154.39	0.72
	Granite	D 4	202.28	98.18	120.49	481.97	0.55	0.70	0.67	1.05	2108.63	0.71
	Quartz Syenite	D 5	188.15	93.68	114.97	459.89	0.51	0.62	0.62	0.78	2012.02	0.69
	Syenite	D 6	255.27	121.08	148.59	594.37	0.69	0.87	0.86	1.49	2600.35	0.87
	Older Trachyte	D 7	264.07	125.15	153.59	614.35	0.71	0.90	0.89	1.55	2687.76	0.90
	Younger Trachyte	D 8	390.88	180.36	221.34	885.36	1.06	1.37	1.32	2.68	3873.46	1.27
	Older Trachyte	D 9	196.05	93.75	115.06	460.23	0.53	0.73	0.66	1.18	2013.49	0.67
	Granite	D 10	189.74	88.57	108.69	434.78	0.51	0.70	0.64	1.28	1902.14	0.63
	Younger Trachyte	D 11	459.44	209.88	257.58	1030.31	1.24	1.60	1.56	3.28	4507.60	1.48
	Mean		273.89	128.84	158.11	632.46	0.74	0.97	0.92	1.73	2767.01	0.92
G. Gabal ElDokhan Do Moghazi (2003)	Granodiorite	Do 1	183.79	88.31	108.37	433.50	0.50	0.69	0.61	1.08	1896.56	0.63
	Rhyolite	Do 2	230.21	111.04	136.27	545.07	0.62	0.81	0.77	1.26	2384.67	0.80
	Rhyolite	Do 3	261.61	124.80	153.16	612.64	0.71	0.92	0.88	1.53	2680.28	0.89
	Biotite Granite	Do 4	287.14	134.39	164.93	659.73	0.78	0.98	0.97	1.80	2886.33	0.96
	Granite	Do 5	302.98	141.21	173.29	693.17	0.82	1.02	1.02	1.94	3032.62	1.01
	Mean		253.14	119.95	147.21	588.82	0.68	0.88	0.85	1.52	2576.09	0.86
G. AlReddah R	Granite	R1	245.26	115.58	141.85	567.40	0.66	0.85	0.83	1.51	2482.36	0.83
	Mean		245.26	115.58	141.85	567.40	0.66	0.85	0.83	1.51	2482.36	0.83

Table 7 (continued)

Localities	Samples		Ra_{eq}	D	AEDE out	AEDE in	H ex	H in	(Iγ)	(I)	(ELCR)	AGDE
	Rock type	ID	$Bq.Kg^{-1}$	$nGy.h^{-1}$	$\mu Sv.y^{-1}$	$\mu Sv.y^{-1}$						$mSv.y^{-1}$
Qattar Q (ElKammar et al. 1997)	Granite	Q 1	352.32	166.73	204.62	818.49	0.95	1.29	1.18	2.20	3580.90	1.19
	Granite	Q 2	227.38	108.16	132.74	530.96	0.61	0.84	0.76	1.40	2322.93	0.77
	Quartz Diorite	Q 3	235.49	111.43	136.75	547.01	0.64	0.86	0.79	1.47	2393.19	0.79
	Granite	Q 4	230.94	109.35	134.20	536.78	0.62	0.85	0.77	1.45	2348.42	0.78
	Granite	Q 5	244.03	115.97	142.33	569.31	0.66	0.93	0.82	1.55	2490.74	0.82
	Granite	Q 6	249.84	116.26	142.68	570.70	0.67	0.88	0.84	1.66	2496.83	0.82
	Granite	Q 7	201.25	95.72	117.47	469.89	0.54	0.70	0.68	1.18	2055.77	0.69
	Granite	Q 8	609.69	278.77	342.11	1368.45	1.65	2.82	2.05	5.23	5986.98	1.90
	Granite	Q 9	365.48	173.12	212.46	849.82	0.99	1.61	1.22	2.63	3717.97	1.21
	Granite	Q 10	4601.65	2127.63	2611.12	10,444.47	12.44	23.65	15.37	40.85	45,694.54	14.35
	Rhyolite	Q 11	199.74	94.77	116.30	465.20	0.54	0.67	0.67	1.16	2035.26	0.68
	Granite	Q 12	272.34	128.10	157.21	628.82	0.74	1.00	0.92	1.76	2751.11	0.91
	Granite	Q 13	48.64	24.10	29.57	118.29	0.13	0.17	0.16	0.22	517.53	0.18
	Mean		602.98	280.78	344.58	1378.32	1.63	2.79	2.02	4.83	6030.17	1.93
Minimum			48.64	24.10	29.57	118.29	0.13	0.17	0.16	0.22	517.53	0.18
Maximum			4601.65	2127.63	2611.12	10,444.47	12.44	23.65	15.37	40.85	45,694.54	14.35
Mean			318.14	149.44	183.40	733.59	0.86	1.25	1.07	2.18	3209.47	1.05

Table 8 Radiological hazard parameters of the Central Eastern Desert rock samples

Localities	Samples		Ra_{eq}	D	AEDEout	AEDEin	H ex	H in	(Iγ)	(I)	(ELCR)	AGDE
	Rock type	ID	$Bq.Kg^{-1}$	$nGy.h^{-1}$	$\mu Sv.y^{-1}$	$\mu Sv.y^{-1}$						$mSv.y^{-1}$
G. Missikat M Awad (2022)	Granite	M 1	184.10	89.02	109.25	437.01	0.50	0.67	0.61	1.02	1911.93	0.64
	Mean		184.10	89.02	109.25	437.01	0.50	0.67	0.61	1.02	1911.93	0.64
G. Gidamy Gd El Mezayen (2017)	Rhyolite	Gd 1	241.35	113.53	139.33	557.31	0.65	0.87	0.81	1.54	2438.21	0.81
	Mean		241.35	113.53	139.33	557.31	0.65	0.87	0.81	1.54	2438.21	0.81
G. DokhanVolcanics (WadiElQueh) Dv (Ressetar and Monrad 1982)	Latite	Dv 1	50.01	24.88	30.54	122.15	0.14	0.18	0.17	0.23	534.41	0.18
	Latite	Dv 2	43.08	21.25	26.08	104.32	0.12	0.14	0.14	0.19	456.42	0.16
	Trachyte	Dv 3	24.49	11.46	14.07	56.28	0.07	0.07	0.08	0.14	246.22	0.08
	Rhyolite	Dv 4	97.98	48.73	59.80	239.19	0.26	0.33	0.32	0.42	1046.45	0.36
	Andesite	Dv 5	6.90	3.50	4.29	17.16	0.02	0.02	0.02	0.02	75.10	0.03
	Andesite	Dv 6	75.23	37.40	45.90	183.58	0.20	0.26	0.25	0.34	803.16	0.27
	Andesite	Dv 7	95.34	46.45	57.01	228.03	0.26	0.34	0.32	0.50	997.64	0.34
	Trachyte	Dv 8	14.30	6.61	8.12	32.46	0.04	0.06	0.05	0.11	142.02	0.05
	Trachyte	Dv 9	13.06	6.37	7.82	31.29	0.04	0.06	0.04	0.08	136.88	0.05
	Andesite	Dv 10	92.23	44.44	54.54	218.15	0.25	0.30	0.31	0.48	954.39	0.32
	Trachy-Andesite	Dv 11	103.91	51.52	63.23	252.92	0.28	0.34	0.34	0.45	1106.53	0.38
	Rhyolite	Dv 12	54.53	26.18	32.13	128.54	0.15	0.18	0.18	0.30	562.36	0.19
	Mean		55.92	27.40	33.63	134.51	0.15	0.19	0.19	0.27	588.46	0.20
G. Abu ElTiyur At (Sidique et al. 2021)	Granite	At 1	157.64	76.47	93.85	375.40	0.43	0.54	0.53	0.81	1642.38	0.55
	Granite	At 2	114.67	57.13	70.11	280.46	0.31	0.39	0.38	0.49	1227.01	0.42
	Granite	At 3	125.19	61.84	75.89	303.58	0.34	0.41	0.42	0.55	1328.14	0.45
	Granite	At 4	138.03	67.96	83.41	333.62	0.37	0.48	0.46	0.65	1459.60	0.50
	Mean		133.88	65.85	80.82	323.26	0.36	0.45	0.44	0.63	1414.28	0.48
Sibai Sb Abdel-Rahman and El-Kibbi (2001)	Granite	Sb 1	238.90	113.42	139.20	556.78	0.65	0.85	0.80	1.44	2435.92	0.81
	Syenite	Sb 2	221.32	104.56	128.32	513.28	0.60	0.79	0.74	1.37	2245.62	0.75
	Mean		230.11	108.99	133.76	535.03	0.62	0.82	0.77	1.41	2340.77	0.78
Um Naggat Un	Granite	Un 1	125.41	62.86	77.14	308.57	0.34	0.41	0.41	0.49	1349.99	0.46
	Syenogranite	Un 2	159.69	78.00	95.73	382.91	0.43	0.55	0.53	0.79	1675.21	0.57
	Granite	Un 3	157.67	77.30	94.86	379.46	0.43	0.52	0.52	0.74	1660.13	0.56
	Granite	Un 4	168.50	82.20	100.88	403.52	0.46	0.57	0.56	0.83	1765.41	0.60
	Granite	Un 5	205.75	98.41	120.78	483.11	0.56	0.75	0.69	1.21	2113.59	0.70
	Granite	Un 6	158.40	77.20	94.75	378.99	0.43	0.55	0.53	0.80	1658.09	0.56
	Granite	Un 7	235.01	113.88	139.75	559.01	0.63	0.88	0.78	1.32	2445.69	0.82
	Granite	Un 8	137.56	67.85	83.27	333.09	0.37	0.43	0.46	0.59	1457.27	0.50
	Granite	Un 9	134.60	67.42	82.74	330.98	0.36	0.43	0.44	0.52	1448.02	0.50
	Granite	Un 10	192.35	91.34	112.10	448.39	0.52	0.70	0.64	1.18	1961.72	0.65
	Mean		167.49	81.65	100.20	400.80	0.45	0.58	0.56	0.85	1753.51	0.59

Table 8 (continued)

Localities	Samples		Ra_{eq}	D	AEDEout	AEDEin	H ex	H in	(Iγ)	(I)	(ELCR)	AGDE
	Rock type	ID	$Bq.Kg^{-1}$	$nGy.h^{-1}$	$\mu Sv.y^{-1}$	$\mu Sv.y^{-1}$						$mSv.y^{-1}$
Abu Dabbab Ad Heikal (2019)	Granite	Ad 1	95.03	47.83	58.70	234.79	0.26	0.32	0.31	0.37	1027.22	0.35
	Granite	Ad 2	22.21	11.01	13.51	54.05	0.06	0.09	0.07	0.11	236.47	0.08
	Granite	Ad 3	129.50	63.06	77.39	309.54	0.35	0.42	0.43	0.63	1354.25	0.46
	Syenite	Ad 4	88.44	44.69	54.84	219.36	0.24	0.30	0.29	0.33	959.69	0.33
	Andesite-Basalt	Ad 5	76.84	36.01	44.19	176.75	0.21	0.40	0.26	0.65	773.28	0.24
	Syenite	Ad 6	91.29	46.46	57.01	228.05	0.25	0.30	0.30	0.31	997.72	0.34
	Mean		83.88	41.51	50.94	203.76	0.23	0.30	0.28	0.40	891.44	0.30
ElBakreya Bk (Abd El-Fatah et al. 2023)	Granite	Bk 1	195.46	93.86	115.18	460.74	0.53	0.72	0.65	1.14	2015.72	0.67
	Granite	Bk 2	166.61	80.38	98.65	394.60	0.45	0.58	0.56	0.90	1726.37	0.58
	Syenite	Bk 3	164.80	79.92	98.08	392.33	0.45	0.59	0.55	0.89	1716.44	0.58
	Granite	Bk 4	144.07	71.26	87.45	349.80	0.39	0.50	0.48	0.66	1530.37	0.52
	Mean		167.73	81.35	99.84	399.37	0.45	0.60	0.56	0.90	1747.23	0.59
Minimum			6.90	3.50	4.29	17.16	0.02	0.02	0.02	0.02	75.10	0.03
Maximum			241.35	113.88	139.75	559.01	0.65	0.88	0.81	1.54	2445.69	0.82
Mean			158.06	76.16	93.47	373.88	0.43	0.56	0.53	0.88	1635.73	0.55

building materials. The poor correlation between ^{232}Th and $^{40}K$from one side and ^{238}U and 40K from the other were attributed to the presence of minerals that greatly affect the mobility of the radionuclides (Stockdale and Bryan 2013). ^{40}K is the most common radionuclide in continental rocks (such as granitic rock) and dominant in many light and non-carbonate minerals (Ergül et al. 2013; Wang et al. 2020). The concentration of ^{40}K showed significant variability, indicating that there are notable differences in ^{40}K levels among the rock samples, due to variations in mineral composition and geochemical characteristics.

Conclusions

The ^{226}Ra, ^{232}Th and ^{40}K activity concentrations in 96 samples of igneous rocks collected at eighteen areas in Egypt allowed estimation of the radium equivalent activity (Ra_{eq}), the absorbed dose rates (*D*), outdoor annual effective dose equivalent ($AEDE_{out}$), the excess lifetime cancer risks (ELCR), internal and external hazard indices (H_{in}) (H_{ex}), annual gonadal dose equivalent (AGDE). Some rocks (samples Q8, Q10, D1, D8, D11 and Gs11) from the Qatar, El Dib, El Garra El Souda areas exhibited values of Ra_{eq} ˃ 370 Bq/kg and H_{ex} ˃1, which are the threshold limits recommended globally, corresponding mainly to high K calc-alkaline granites. The index of gamma radiation has been related to the effective dose rate, indicating that the radioactivity emitted in all studied samples did not exceed the guideline value of 1 mSv/yr. The exhalation rate of Rn and daughters varied between < 1, except for one sample from Qatar (Q10).

The results reported here suggest that most of the studied igneous rocks can be utilized in closed indoor environments. In contrast, those exhibiting values of Raeq ˃370 Bq/kg and Hex ˃1 could be used in outdoor environments and indoors with ample ventilation to avoid any risk of human exposure to ^{222}Rn and daughters due to their radiotoxicity.

Table 9 Radiological hazard parameters of the Southeastern Desert rock samples

Localities	Samples		Ra_{eq}	D	AEDEout	AEDEin	H ex	H in	(Iγ)	(I)	(ELCR)	AGDE
	Rock type	ID	$Bq.Kg^{-1}$	$nGy.h^{-1}$	$\mu Sv.y^{-1}$	$\mu Sv.y^{-1}$						$mSv.y^{-1}$
Hamash H (Gharib et al. 2021)	Andesite-Basalt	H 1	30.11	13.54	16.62	66.49	0.08	0.12	0.10	0.25	290.88	0.09
	Andesite	H 2	59.14	28.05	34.42	137.67	0.16	0.21	0.20	0.36	602.32	0.20
	Andesite	H 3	32.17	15.76	19.34	77.38	0.09	0.11	0.11	0.16	338.52	0.11
	Basalt	H 4	32.55	14.74	18.09	72.36	0.09	0.13	0.11	0.27	316.57	0.10
	Andesite-Basalt	H 5	47.86	22.72	27.88	111.52	0.13	0.18	0.16	0.30	487.90	0.16
	Basalt	H 6	2.08	0.96	1.17	4.69	0.01	0.01	0.01	0.02	20.54	0.01
	Trachy-Basalt	H 7	9.27	4.19	5.14	20.55	0.03	0.04	0.03	0.08	89.92	0.03
	Trachyte	H 8	34.63	16.12	19.79	79.14	0.09	0.13	0.12	0.24	346.26	0.11
	Mean		30.98	14.51	17.81	71.23	0.08	0.12	0.10	0.21	311.61	0.10
Minimum			2.08	0.96	1.17	4.69	0.01	0.01	0.01	0.02	20.54	0.01
Maximum			59.14	28.05	34.42	137.67	0.16	0.21	0.20	0.36	602.32	0.20
Mean			30.98	14.51	17.81	71.23	0.08	0.12	0.10	0.21	311.61	0.10

Table 10 Radiological Hazard parameters of the studied rock samples from the Southwestern Desert

Localities	Samples		Ra_{eq}	D	AEDEout	AEDEin	Hex	Hin	(Iγ)	(I)	(ELCR)	AGDE
	Rock Type	ID	$Bq.Kg^{-1}$	$nGy.h^{-1}$	$\mu Sv.y^{-1}$	$\mu Sv.y^{-1}$						$mSv.y^{-1}$
ElGarraElHamra Gh	Quartz Syenite	Gh 1	218.92	104.92	128.77	515.07	0.59	0.74	0.73	1.21	2253.42	0.76
	Syenite	Gh 2	140.08	69.18	84.90	339.59	0.38	0.50	0.46	0.66	1485.72	0.50
	Mean		179.50	87.05	106.83	427.33	0.48	0.62	0.60	0.93	1869.57	0.63
ElGarraElSouda Gs	Syenite	Gs 1	576.16	268.67	329.72	1318.90	1.56	2.05	1.94	3.80	5770.17	1.90
	Syenite	Gs 2	216.90	105.57	129.56	518.22	0.59	0.79	0.72	1.15	2267.23	0.76
	Latite	Gs 3	342.18	157.56	193.36	773.43	0.92	1.18	1.16	2.34	3383.77	1.11
	Latite	Gs 4	64.52	32.25	39.58	158.30	0.17	0.21	0.21	0.26	692.58	0.24
	Quartz Syenite	Gs 5	165.14	82.95	101.80	407.20	0.45	0.55	0.54	0.64	1781.49	0.61
	Syenite	Gs 6	316.75	148.65	182.42	729.70	0.86	1.09	1.07	1.98	3192.42	1.06
	Granite	Gs 7	198.15	97.25	119.35	477.40	0.54	0.68	0.66	0.95	2088.64	0.71
	Granite	Gs 8	205.55	98.79	121.24	484.95	0.56	0.69	0.69	1.11	2121.64	0.71
	Latite	Gs 9	20.62	10.65	13.07	52.26	0.06	0.07	0.07	0.06	228.66	0.08
	Mean		234.00	111.37	136.68	546.71	0.63	0.81	0.78	1.37	2391.84	0.80
Um Shagher Us Assran (2015)	Syenite	Us 1	298.27	139.97	171.77	687.10	0.81	1.02	1.01	1.86	3006.05	1.00
	Granite	Us 2	295.30	137.69	168.97	675.90	0.80	1.02	1.00	1.91	2957.06	0.98
	Mean		296.78	138.83	170.37	681.50	0.80	1.02	1.00	1.88	2981.56	0.99
Bir Sa(fsaf Sf Assran (2015)	Granite	Sf 1	279.74	130.80	160.52	642.10	0.76	0.99	0.94	1.82	2809.19	0.93
	Granite	Sf 2	237.08	112.22	137.72	550.90	0.64	0.87	0.80	1.49	2410.18	0.80
	Granite	Sf 3	238.48	113.71	139.55	558.20	0.64	0.83	0.80	1.39	2442.11	0.82
	Mean		251.77	118.91	145.93	583.73	0.68	0.90	0.85	1.57	2553.83	0.85
Minimum			20.62	10.65	13.07	52.26	0.06	0.07	0.07	0.06	228.66	0.08
Maximum			576.16	268.67	329.72	1318.90	1.56	2.05	1.94	2.34	5770.17	1.90
Mean of WD			240.51	114.04	139.95	559.82	0.65	0.84	0.81	1.44	2449.20	0.82

Table 11 Major oxides (wt%), trace and rare earth elements (ppm) concentration for some of the studied rock samples

Samples ID	SiO_2	TiO_2	Al_2O_3	Fe_2O_3	MnO	MgO	CaO	Na_2O	K_2O	P_2O_5	LOI	Cs	V	Cr
	%	%	%	%	%	%	%	%	%	%	%	ppm	ppm	ppm
Mo 1	77.6	0.18	11.75	1.09	0.1	0.08	0.45	3.96	4	0.01	0.22	1.9	6	10
Mo 2	76.6	0.09	12.15	0.67	0.03	0.08	0.28	3.99	4.29	0.01	0.44	1.7	<5	<10
D 1	70.1	0.13	14.5	2.16	0.03	0.1	0.6	4.83	5.56	0.01	0.31	1.31	6	<10
D 8	73.1	0.16	13.6	2.31	0.03	0.18	0.67	4.29	4.96	0.01	0.94	1.59	6	<10
D 9	68.6	0.49	14.95	3.46	0.05	0.97	1.83	4.72	3.81	0.15	0.88	1.8	52	10
Do 2	75.1	0.23	12.15	1.92	0.03	0.11	0.41	3.41	5.5	0.02	0.44	1.92	7	<10
Do 3	76.6	0.19	12.1	1.59	0.03	0.18	0.33	3.29	5.21	0.01	0.45	1.86	7	<10
Do 5	73.6	0.25	14.15	1.57	0.03	0.33	1.23	3.75	5.09	0.07	0.77	5.4	14	<10
R 1	73.1	0.32	14.1	2.22	0.04	0.46	1.42	3.94	4.96	0.09	0.36	2.89	21	<10
Q 1	78.3	0.05	12.35	1.12	0.02	0.03	0.34	4.43	4.27	<0.01	0.4	5.61	<5	<10
Q 2	78.3	0.04	11.4	0.95	<0.01	0.03	0.39	4.01	4.1	<0.01	0.37	1.4	<5	<10
Q 5	78.1	0.04	12.15	1.5	0.02	0.02	0.38	4.3	4.24	<0.01	0.64	2.4	<5	<10
Q 6	78.9	0.05	11.2	1.26	0.01	0.04	0.31	4.13	3.65	<0.01	0.54	0.63	5	<10
Q 8	77.3	0.04	12.4	1.08	<0.01	0.04	0.39	4.35	4.23	0.01	0.59	2.09	<5	<10
Q 9	76	0.05	12.2	1.13	0.02	0.05	0.43	4.17	4.24	<0.01	0.76	1.95	<5	<10
Q 10	76	0.04	12.35	1.63	0.03	0.08	0.4	4.08	4.29	<0.01	0.9	2.06	<5	<10
Q 11	75.7	0.05	12	1.68	0.01	0.04	0.34	4.24	4.34	<0.01	0.38	4.17	<5	<10
Q 12	75.6	0.04	12.6	1.2	0.05	0.04	0.43	4.42	4.54	<0.01	0.53	2.66	<5	<10
NED Mean	75.48	0.14	12.67	1.59	0.03	0.16	0.59	4.13	4.52	0.04	0.55	2.41	13.78	10
NED SD	2.84	0.12	1.09	0.66	0.02	0.23	0.44	0.39	0.56	0.05	0.22	1.35	15.26	0
M 1	77.1	0.09	12.85	0.59	0.05	0.07	0.52	4.23	4.44	0.03	0.3	1.87	<5	<10
Gd 1	75.4	0.13	12.25	1.65	0.04	0.13	0.75	3.85	4.31	0.02	0.45	3.81	6	<10
Dv 1	61.4	0.74	15.6	5.32	0.09	3.17	4.11	4.7	1.57	0.17	2.75	1.9	121	80
Dv 4	72.4	0.44	12.9	2.55	0.03	0.79	2.19	3.06	3.06	0.09	2.73	0.68	54	10
Dv 6	57.6	0.94	14.3	6.87	0.12	3.39	4.82	2.4	2.22	0.24	5.17	2.29	120	90
Dv 7	60.4	0.94	15.05	7.36	0.12	3.65	2.75	2.66	2.22	0.24	3.92	2.02	153	90
Dv 12	86.9	0.74	2.78	2.52	0.03	0.36	0.75	1.33	1.1	0.02	3.49	0.76	23	100
At 1	80.1	0.16	10.6	2.22	0.04	0.04	0.32	3.38	4.34	<0.01	0.24	0.16	<5	10
At 2	76.3	0.14	11.2	2.05	0.04	0.08	0.41	3.58	4.37	0.01	0.56	0.53	<5	<10
At 3	72.7	0.18	13.05	2.3	0.04	0.18	1.08	4.37	4.01	0.04	0.47	0.53	<5	<10
At 4	76.7	0.08	12.45	0.69	0.01	0.11	0.17	3.76	4.56	<0.01	1.08	0.56	<5	<10
Sb 1	69.5	0.47	12.85	5.6	0.13	0.45	0.76	6.08	4.75	0.12	1.1	0.83	17	<10
Sb 2	66.7	0.64	12.3	6.6	0.16	0.73	1.13	6.13	4.3	0.14	1.51	0.54	14	<10
Un 1	74.7	0.14	12	1.92	0.03	0.07	0.36	3.94	4.71	0.01	0.35	0.56	<5	<10
Un 5	73.6	0.32	12.8	3.31	0.06	0.22	1.11	4.13	4.26	0.04	0.38	0.38	8	<10
Un 7	74	0.07	14.8	0.88	<0.01	0.09	0.18	4.6	5.4	<0.01	0.92	1.57	<5	<10
Ad 1	76.3	0.19	12.85	1.87	0.02	0.18	1.05	4.49	3.28	0.03	0.28	0.63	9	<10
Ad 3	74.6	0.24	13.3	1.87	0.03	0.35	1.13	4.29	3.79	0.04	0.35	1.7	13	<10
Ad 5	54.3	0.05	1.51	5.67	0.21	20.2	11.9	0.21	0.02	<0.01	3.57	0.01	118	3230
Bk 1	78	0.04	12.7	0.72	0.04	0.06	0.55	4.33	4.14	<0.01	0.6	2.49	<5	<10
Bk 2	77.8	0.03	13.35	0.56	0.03	0.05	0.46	4.84	4.06	<0.01	0.59	1.95	<5	<10
Bk 3	63.7	0.33	15.5	5.21	0.33	0.24	2.07	5.4	3.74	0.05	3.25	0.15	<5	<10
CED Mean	71.83	0.32	12.14	3.11	0.08	1.57	1.75	3.9	3.58	0.08	1.55	1.18	54.67	515.71
CED SD	8	0.3	3.48	2.24	0.08	4.31	2.58	1.38	1.35	0.08	1.5	0.97	56.24	1197.5
H 1	56	0.98	15.85	7.64	0.13	3.92	6.71	3.89	0.45	0.21	2.49	0.34	193	80
H 2	63.1	0.61	14.8	5.7	0.1	3.77	3.37	3.51	0.99	0.12	3.35	0.52	114	140
H 6	48.5	1.23	14.1	12	0.2	1.58	18.7	0.05	0.02	0.15	1.86	0.02	428	110
SED Mean	55.87	0.94	14.92	8.45	0.14	3.09	9.59	2.48	0.49	0.16	2.57	0.29	245	110
SED SD	7.3	0.31	0.88	3.23	0.05	1.31	8.06	2.12	0.49	0.05	0.75	0.25	163.33	30
Gs 2	64.7	1.12	15.7	4.99	0.15	0.22	1.43	5.99	5.35	0.15	0.71	0.95	<5	30
Gs 4	45.8	3.76	13.3	16.7	0.49	0.47	7.9	2.86	2.32	1.21	4.91	1.45	209	30
Us 2	72.6	0.32	14.8	2.46	0.04	0.63	1.8	3.69	4.76	0.1	0.42	1.07	30	<10
Sf 2	77.5	0.11	12.95	1.18	0.02	0.19	1.05	3.53	4.43	0.02	0.33	1.89	7	<10
Sf 3	76.5	0.12	13.1	1.11	0.02	0.19	1.19	3.45	4.66	0.03	0.3	0.73	9	<10
SWD (Mean)	67.42	1.09	13.97	5.29	0.14	0.34	2.67	3.9	4.3	0.3	1.33	1.22	63.75	30
SWD SD	13.09	1.55	1.22	6.57	0.2	0.2	2.94	1.21	1.16	0.51	2.01	0.46	97.39	0

Samples ID	Ga	Rb	Sr	Y	Zr	Nb	Sn	Ba	Hf	Ta	W	Th	U
	ppm	ppm	ppm	ppm	ppm	ppm	ppm	ppm	ppm	ppm	ppm	ppm	ppm
Mo 1	16.4	141.5	32.8	16.3	91	24.3	2	103	4.8	2.6	2	20.2	7.1
Mo 2	15.8	145	57.3	10.5	70	12.2	1	205	3.4	1.6	2	13.95	4.06
D 1	30.5	269	93.6	68.2	628	166	3	203	18.1	10.5	2	56.8	19.5
D 8	22.8	282	60	35.2	259	74.8	4	176	8.2	8.6	24	47.6	12.05
D 9	19.5	117.5	400	18.1	217	16.6	2	686	6.1	1.3	3	14.95	6.92
Do 2	19.6	139	66.5	29.5	343	27.9	2	107	10	1.9	8	16.1	4.5
Do 3	18.3	206	58.9	27.1	197	23.1	2	123	6.8	2.2	2	27.9	9.24
Do 5	19.9	204	219	21.3	209	15.4	1	736	6.1	1.7	1	27.8	4.08
R 1	21.8	175.5	200	40.5	279	21.9	3	565	8.2	1.9	1	17.2	4.87
Q 1	31.8	257	5.6	113	160	88.9	11	17.9	10.7	6.4	3	25.5	9.23
Q 2	28.3	196	13.3	77	129	71.8	10	27.9	8.8	5.7	3	20.3	7.49
Q 5	30.4	249	6.6	92.1	155	90	10	11.9	10.6	6.2	3	20	8.88
Q 6	21.3	119.5	33.3	89.6	150	73.9	8	39.3	10.7	6	3	16.2	4.8
Q 8	31.4	235	9.2	78.8	189	121	15	17.7	11	6.1	4	22	47.5
Q 9	30.9	238	11.8	118	164	116.5	16	18	10.9	6.3	4	23.5	36.8
Q 10	31.1	245	12.4	133	174	84.6	16	26.6	10.2	6.2	5	19.05	492
Q 11	30.5	254	6.5	102.5	132	120.5	12	17.7	8.6	6.9	3	18.8	4.92
Q 12	32.3	256	10.5	131.5	185	90	13	15	11.1	5.9	3	26.1	15.1
NED Mean	25.14	207.17	72.07	66.79	207.28	68.86	7.28	172	9.13	4.89	4.22	24.11	38.84
NED SD	6.09	54.81	103.17	42.58	123.59	45.67	5.6	237.02	3.23	2.72	5.19	11.17	113.71
M 1	17.7	142.5	43.5	31.9	79	11	1	202	4.2	1	1	18.45	8.6
Gd 1	23.3	209	50.4	62.2	205	26.4	7	168	7.6	3.6	2	23.7	9.47
Dv 1	19.3	33.2	281	15.8	153	4.3	2	396	4.1	0.2	2	3.2	1.15
Dv 4	16	79.5	101.5	21.4	207	4.4	1	249	6.4	0.3	2	6.97	1.84
Dv 6	19.9	61.1	192.5	39.9	238	12.6	2	418	6.3	0.8	2	5.86	2.22
Dv 7	21.2	63.5	201	43.1	269	13.8	3	418	7.4	0.9	2	6.42	2.59
Dv 12	4.5	25.5	195.5	10.4	396	8.4	<1	275	9.4	0.5	7	5.66	1.05
At 1	24.6	43	12.9	59.7	539	42.1	2	625	14.2	1.7	1	5.41	1.48
At 2	25.2	57.2	19.3	68	408	34.6	3	398	12	2.3	1	8.73	3.08
At 3	24.4	73.5	108.5	47.6	338	35.2	4	598	9.5	2.4	1	6.39	2.84
At 4	34.8	106.5	9.3	106	242	57	4	67.3	8.3	2.4	2	6.19	3.16
Sb 1	37.3	130	91.4	134.5	1560	179.5	13	481	39.2	11.8	2	24.8	6.24
Sb 2	38.1	114.5	86.2	135	1570	173	13	501	37.7	11.1	1	23	6.76
Un 1	26.8	71.2	27.9	96.8	316	33.4	3	260	9.8	2	2	10.4	3.84
Un 5	26.3	50.9	70.1	73.3	558	35.7	3	575	13.4	1.8	1	13.95	1.99
Un 7	40.4	264	13	114.5	556	194	18	87.1	35.8	11.3	3	16.9	12.15
Ad 1	18.2	54.3	70.9	34.1	197	7.1	4	504	5.8	0.5	1	5.13	1.37
Ad 3	18	93.4	68.2	32.8	280	5.7	3	406	7.9	0.4	1	10.95	2.52
Ad 5	2.5	0.2	14.5	3.8	<2	0.8	1	2.7	0.1	<0.1	1	<0.05	0.14
Bk 1	24.5	199.5	10.7	60.7	98	18.4	7	29	5.4	1.6	1	12.3	5.94
Bk 2	25.7	204	9.2	31.5	75	15.5	5	19.7	4.6	1.2	1	8.21	3.93
Bk 3	30.5	73	159.5	58.4	764	105	5	711	17.5	6.2	2	11.85	3.67
CED Mean	23.6	97.7	83.5	58.25	430.86	46.27	4.95	335.95	12.12	3.05	1.77	10.66	3.91
CED SD	9.47	68.12	77.32	38.24	416.34	59.96	4.49	213.25	11.04	3.75	1.31	6.87	3.07
H 1	19.1	7.5	450	17.3	107	3	1	159.5	2.9	0.1	1	1.53	0.63
H 2	19.3	24.3	213	24.8	159	6	1	193.5	4.4	0.4	2	3.86	1.28
H 6	25.3	0.3	578	27.2	71	1.8	2	17.8	2	<0.1	2	0.22	0.59
SED Mean	21.23	10.7	413.67	23.1	112.33	3.6	1.33	123.6	3.1	0.25	1.67	1.87	0.83
SED SD	3.52	12.32	185.19	5.16	44.24	2.16	0.58	93.19	1.21	0.21	0.58	1.84	0.39
Gs 2	24.8	62.1	44.2	20.6	417	56.2	2	337	8.7	2.7	1	7.69	1.7
Gs 4	20	52	656	27.1	186	32.8	1	902	4.3	1.5	2	2.45	1.83
Us 2	18.8	138.5	263	17.5	257	7.4	1	1060	6.8	0.5	2	16.6	2.6
Sf 2	17.8	166.5	96.8	9.7	93	7.7	1	309	2.9	0.4	1	19.3	7.47
Sf 3	17.9	141.5	93.3	17.4	112	6.4	1	261	3.9	0.5	1	21.5	5.98
SWD (Mean)	19.86	112.12	230.66	18.46	213	22.1	1.2	573.8	5.32	1.12	1.4	13.51	3.92
SWD SD	2.9	51.56	251.75	6.29	131.23	22.06	0.45	376.88	2.37	0.99	0.55	8.11	2.64

Samples ID	La	Ce	Pr	Nd	Sm	Eu	Gd	Tb	Dy	Ho	Er	Tm	Yb	Lu
	ppm	ppm	ppm	ppm	ppm	ppm	ppm	ppm	ppm	ppm	ppm	ppm	ppm	ppm
Mo 1	19	37.1	4.42	14.7	2.74	0.24	2.29	0.37	2.32	0.52	1.7	0.27	2.01	0.36
Mo 2	14.5	37.7	3.16	10.4	2.01	0.25	1.54	0.25	1.55	0.34	1.11	0.18	1.36	0.23
D 1	142	228	22.7	69.2	11.85	0.39	10.2	1.76	10.65	2.28	6.77	1	6.05	0.91
D 8	72.8	124.5	12.25	37.3	6.12	0.52	4.98	0.85	5.19	1.14	3.45	0.58	3.79	0.63
D 9	30.5	53.4	6.38	22.2	4.13	0.77	3.3	0.49	2.78	0.58	1.65	0.25	1.61	0.27
Do 2	35.6	116	10.75	38.4	6.84	0.36	5.12	0.86	5.1	1.05	3.15	0.47	3.08	0.51
Do 3	51	104.5	12.35	41.5	7.13	0.48	5.31	0.81	4.6	0.91	2.52	0.37	2.51	0.41
Do 5	54.9	104	11.45	38.1	6.17	0.96	4.39	0.65	3.44	0.68	1.93	0.28	1.82	0.29
R 1	43.2	88.2	11.45	41.9	8.23	1.14	6.67	1.11	6.31	1.33	3.94	0.59	3.75	0.62
Q 1	13.2	40.6	6.89	30.7	11.75	0.08	13.35	2.59	16.25	3.42	10.15	1.5	9.45	1.43
Q 2	10.2	27.9	5.29	24.5	9.36	0.06	9.65	1.71	10.45	2.21	6.6	1.02	6.64	1.03
Q 5	11.4	34.8	6.05	27.8	10.7	0.06	12.75	2.29	13.55	2.81	8.12	1.22	7.82	1.2
Q 6	12.9	29.4	6.3	27.7	10.15	0.08	12.2	2.23	13.6	2.82	8.06	1.19	7.58	1.14
Q 8	13.3	38.9	6.57	30	11.3	0.09	12.7	2.11	12.4	2.53	7.44	1.11	7.18	1.1
Q 9	14.1	43.6	7.38	33.3	12.55	0.09	15	2.73	17.15	3.64	10.55	1.55	9.42	1.42
Q 10	15.1	40.7	7.32	33.4	12.1	0.09	14.35	2.72	17.6	3.82	10.8	1.49	8.83	1.35
Q 11	13.5	39.5	6.65	29.8	11.4	0.08	13.4	2.49	15.05	3.1	8.96	1.29	8.01	1.18
Q 12	14.2	42.5	7.48	34.1	13.45	0.08	15.95	2.96	18.65	3.91	10.9	1.58	9.56	1.47
NED Mean	32.3	68.41	8.6	32.5	8.78	0.32	9.06	1.61	9.81	2.06	5.99	0.89	5.58	0.86
NED SD	32.99	51.34	4.45	12.48	3.51	0.33	4.82	0.93	5.92	1.25	3.55	0.51	3.05	0.45
M 1	177	343	39.9	128	20.4	0.46	11.9	1.35	5.81	0.95	2.08	0.3	1.86	0.3
Gd 1	31.6	68	8.74	31.6	6.93	0.54	6.44	1.25	7.96	1.83	5.99	0.99	6.91	1.14
Dv 1	16	32.9	4.3	16.7	3.32	1.06	3.15	0.46	2.71	0.55	1.52	0.21	1.3	0.21
Dv 4	16.9	37.5	5.17	20.7	4.53	0.6	3.79	0.59	3.4	0.7	2.08	0.32	2.17	0.34
Dv 6	29.8	60.3	8.34	33.5	7.01	1.6	6.8	1.09	6.45	1.38	3.88	0.54	3.53	0.57
Dv 7	31.7	65.6	9.01	35.6	7.77	1.68	7.25	1.16	6.96	1.48	4.26	0.62	3.92	0.63
Dv 12	17.7	35	4.29	15.3	2.74	0.51	2.03	0.33	1.97	0.41	1.29	0.21	1.39	0.25
At 1	70.1	158.5	19.65	75.4	14.95	2.07	12.15	1.88	10.7	2.16	5.88	0.83	5.21	0.85
At 2	56.7	130	16.35	64.4	14.5	1.86	13.05	2.02	11.35	2.35	6.4	0.89	5.31	0.9
At 3	16.6	37.3	5.45	23.9	6.48	1.93	6.61	1.18	7.24	1.56	4.51	0.7	4.49	0.73
At 4	55.3	106.5	17.05	67.5	20.2	1.15	20.9	3.33	18.15	3.44	8.8	1.14	6.31	0.88
Sb 1	157.5	294	34.2	119.5	23.1	3.82	20.7	3.51	21.5	4.51	13.2	1.94	12.2	1.89
Sb 2	183	337	37.9	132	24.8	4.1	21.4	3.59	21.6	4.6	13.35	1.94	12.1	1.87
Un 1	52.7	122.5	16.65	68.1	17.05	1.18	17.45	3	18.05	3.65	10.2	1.4	8.23	1.3
Un 5	208	402	48.5	177.5	28.1	2.44	20.6	2.74	14.85	2.83	7.78	1.04	6.65	1.02
Un 7	4.3	7.5	1.21	4.7	2.08	0.05	3.64	1.27	12.05	3.24	12.4	2.27	16.9	2.64
Ad 1	22.6	45.6	6.23	24.5	5.39	0.65	5	0.82	5.43	1.16	3.57	0.5	3.43	0.51
Ad 3	20.9	53	5.7	21.7	4.72	0.59	4.63	0.79	5.15	1.11	3.37	0.52	3.42	0.51
Ad 5	0.9	1.4	0.23	1	0.26	0.32	0.43	0.06	0.42	0.09	0.27	0.04	0.21	0.03
Bk 1	8.6	21.8	3.46	13.7	3.87	0.15	4.67	0.88	6.15	1.5	5.27	0.88	6.38	1.05
Bk 2	3.5	10.2	1.53	6.2	1.98	0.1	2.29	0.48	3.77	0.92	3.39	0.58	4.4	0.72
Bk 3	98.3	197	23.4	88.9	16.55	4.04	13.15	1.91	10.7	2.1	5.8	0.79	4.8	0.72
CED Mean	58.17	116.66	14.42	53.2	10.76	1.4	9.46	1.53	9.2	1.93	5.7	0.85	5.51	0.87
CED SD	64.42	121.54	14.06	49.03	8.53	1.25	6.96	1.08	6.24	1.29	3.84	0.59	4	0.62
H 1	10.8	25.1	3.72	16.8	3.68	1.13	3.53	0.49	2.99	0.62	1.77	0.24	1.54	0.24
H 2	17.5	36.9	4.99	21.1	4.49	1.02	4.29	0.65	4.17	0.84	2.58	0.37	2.33	0.37
H 6	3.8	9.9	1.72	9	2.94	0.98	3.87	0.65	4.32	0.96	2.83	0.4	2.68	0.4
SED Mean	10.7	23.97	3.48	15.63	3.7	1.04	3.9	0.6	3.83	0.81	2.39	0.34	2.18	0.34
SED SD	6.85	13.54	1.65	6.13	0.78	0.08	0.38	0.09	0.73	0.17	0.55	0.09	0.58	0.09
Gs 2	27	55.5	7.18	27.8	5.48	2.23	4.44	0.64	3.75	0.75	2.29	0.34	2.41	0.36
Gs 4	30.2	61.9	8.54	37.5	8.05	2.9	7.65	0.97	5.12	0.94	2.25	0.27	1.47	0.2
Us 2	47.5	89.5	10.5	36.5	5.84	0.85	4.16	0.57	3.16	0.61	1.67	0.23	1.45	0.21
Sf 2	14.1	27.4	3.37	12.8	2.59	0.52	2.06	0.27	1.56	0.31	0.94	0.12	0.75	0.11
Sf 3	23.6	48.9	6.18	23.2	4.68	0.49	3.61	0.51	2.88	0.59	1.62	0.22	1.56	0.23
SWD (Mean)	28.48	56.64	7.15	27.56	5.33	1.4	4.38	0.59	3.29	0.64	1.75	0.24	1.53	0.22
SWD SD	12.22	22.49	2.66	10.19	1.98	1.1	2.04	0.25	1.3	0.23	0.55	0.08	0.59	0.09

Table 12 Pearson correlation between rare earth elements, trace elements and major oxides

	SiO2	TiO2	Al2O3	Fe2O3	MnO	MgO	CaO	Na2O	K2O	P2O5	LOI	Cs	V	Cr	Ga	Rb	Sr
SiO2	1.00																
TiO2	-0.72	1.00															
Al2O3	-0.25	0.17	1.00														
Fe2O3	-0.91	0.90	0.15	1.00													
MnO	-0.79	0.80	0.07	0.86	1.00												
MgO	-0.51	0.06	-0.49	0.30	0.30	1.00											
CaO	-0.81	0.51	-0.08	0.75	0.59	0.57	1.00										
Na2O	0.31	-0.22	0.51	-0.32	-0.15	-0.52	-0.67	1.00									
K2O	0.62	-0.43	0.26	-0.61	-0.43	-0.61	-0.76	0.64	1.00								
P2O5	-0.70	0.96	0.18	0.83	0.80	0.23	0.44	-0.17	-0.34	1.00							
LOI	-0.70	0.65	-0.09	0.73	0.67	0.48	0.54	-0.45	-0.73	0.61	1.00						
Cs	0.26	-0.16	0.14	-0.29	-0.28	-0.22	-0.29	0.16	0.33	-0.02	-0.22	1.00					
V	-0.84	0.61	0.14	0.82	0.63	0.30	0.92	-0.59	-0.75	0.48	0.57	-0.29	1.00				
Cr	-0.23	-0.29	-0.68	-0.05	0.19	0.97	0.40	-0.53	-0.44	-0.34	0.15	-0.37	-0.07	1.00			
Ga	0.11	-0.16	0.43	-0.10	-0.03	-0.46	-0.29	0.60	0.49	-0.02	-0.31	0.14	-0.04	-0.68	1.00		
Rb	0.52	-0.45	0.14	-0.56	-0.45	-0.40	-0.53	0.40	0.67	-0.31	-0.54	0.64	-0.61	-0.41	0.49	1.00	
Sr	-0.73	0.79	0.30	0.81	0.61	0.09	0.68	-0.35	-0.56	0.71	0.55	-0.15	0.78	-0.39	-0.26	-0.48	1.00
Y	0.26	-0.27	0.02	-0.20	-0.15	-0.29	-0.35	0.43	0.38	-0.09	-0.27	0.16	-0.24	-0.46	0.85	0.47	-0.44
Zr	-0.09	0.04	-0.02	0.19	0.25	-0.08	-0.14	0.47	0.22	-0.03	0.05	-0.30	-0.25	-0.36	0.48	-0.10	-0.09
Nb	0.14	-0.17	0.09	-0.11	0.05	-0.24	-0.31	0.54	0.44	-0.05	-0.20	0.08	-0.29	-0.30	0.81	0.53	-0.34
Sn	0.31	-0.28	-0.07	-0.25	-0.16	-0.23	-0.31	0.40	0.29	-0.13	-0.23	0.26	-0.27	-0.31	0.77	0.60	-0.42
Ba	-0.26	0.43	0.28	0.36	0.36	-0.11	0.01	0.13	0.05	0.42	0.20	-0.15	-0.11	-0.44	-0.14	-0.39	0.47
Hf	0.11	-0.10	0.08	-0.02	0.08	-0.23	-0.30	0.52	0.38	-0.09	-0.12	-0.12	-0.32	-0.49	0.69	0.22	-0.24
Ta	0.09	-0.21	0.00	-0.09	0.05	-0.33	-0.36	0.57	0.43	-0.11	-0.20	0.09	-0.35	-0.56	0.79	0.59	-0.36
W	0.13	-0.07	-0.08	-0.09	-0.13	-0.10	-0.12	-0.02	0.12	-0.10	0.00	0.06	-0.14	-0.24	0.00	0.33	-0.08
Th	0.34	-0.40	0.00	-0.39	-0.30	-0.42	-0.41	0.35	0.62	-0.32	-0.45	0.37	-0.55	-0.50	0.30	0.78	-0.37
U	0.11	-0.11	-0.02	-0.11	-0.10	-0.07	-0.10	0.05	0.09	-0.20	-0.07	0.08	-0.47	-0.32	0.19	0.26	-0.14
La	0.01	-0.01	0.11	0.06	0.10	-0.16	-0.19	0.37	0.31	-0.10	-0.12	-0.20	-0.33	-0.41	0.28	-0.05	-0.08
Ce	0.04	-0.03	0.10	0.04	0.08	-0.18	-0.21	0.36	0.33	-0.11	-0.14	-0.19	-0.34	-0.39	0.28	-0.06	-0.11
Pr	0.06	-0.03	0.09	0.03	0.08	-0.19	-0.22	0.36	0.32	-0.09	-0.14	-0.19	-0.32	-0.41	0.33	-0.07	-0.13
Nd	0.05	-0.02	0.09	0.05	0.10	-0.21	-0.22	0.36	0.31	-0.06	-0.12	-0.20	-0.29	-0.42	0.37	-0.09	-0.13
Sm	0.15	-0.10	0.05	-0.04	0.03	-0.27	-0.30	0.40	0.35	-0.05	-0.18	-0.11	-0.26	-0.44	0.58	0.06	-0.26
Eu	-0.44	0.46	0.21	0.56	0.61	-0.02	0.13	0.27	-0.05	0.37	0.35	-0.39	0.14	-0.40	0.23	-0.49	0.30
Gd	0.17	-0.13	0.03	-0.07	-0.02	-0.28	-0.30	0.40	0.34	-0.02	-0.19	-0.04	-0.21	-0.46	0.71	0.17	-0.32
Tb	0.22	-0.20	0.01	-0.13	-0.08	-0.29	-0.33	0.42	0.36	-0.06	-0.23	0.04	-0.23	-0.46	0.78	0.29	-0.38
Dy	0.23	-0.22	0.02	-0.15	-0.10	-0.29	-0.33	0.43	0.37	-0.07	-0.24	0.06	-0.22	-0.46	0.82	0.34	-0.40
Ho	0.23	-0.24	0.03	-0.16	-0.11	-0.29	-0.34	0.44	0.38	-0.08	-0.25	0.08	-0.22	-0.46	0.85	0.38	-0.41
Er	0.24	-0.26	0.04	-0.18	-0.13	-0.29	-0.34	0.45	0.39	-0.11	-0.26	0.11	-0.24	-0.47	0.87	0.43	-0.43
Tm	0.26	-0.28	0.05	-0.21	-0.15	-0.29	-0.35	0.46	0.40	-0.13	-0.27	0.13	-0.26	-0.47	0.87	0.47	-0.44
Yb	0.27	-0.28	0.07	-0.23	-0.17	-0.29	-0.35	0.46	0.41	-0.15	-0.28	0.15	-0.27	-0.48	0.85	0.49	-0.44
Lu	0.28	-0.29	0.06	-0.23	-0.18	-0.29	-0.36	0.46	0.41	-0.17	-0.28	0.15	-0.28	-0.47	0.84	0.49	-0.45

	Y	Zr	Nb	Sn	Ba	Hf	Ta	W	Th	U	La	Ce	Pr	Nd	Sm	Eu	Gd	Tb	Dy	Ho	Er	Tm	Yb	Lu
Y	1.00																							
Zr	0.44	1.00																						
Nb	0.79	0.62	1.00																					
Sn	0.86	0.29	0.80	1.00																				
Ba	-0.28	0.33	-0.18	-0.40	1.00																			
Hf	0.67	0.89	0.84	0.60	0.11	1.00																		
Ta	0.75	0.58	0.97	0.77	-0.27	0.79	1.00																	
W	0.02	-0.05	0.15	0.13	-0.19	0.01	0.29	1.00																
Th	0.29	0.19	0.53	0.30	-0.20	0.29	0.64	0.43	1.00															
U	0.33	-0.06	0.16	0.39	-0.18	0.03	0.18	0.12	0.11	1.00														
La	0.24	0.68	0.33	-0.04	0.35	0.52	0.31	-0.02	0.33	-0.08	1.00													
Ce	0.26	0.67	0.31	-0.03	0.34	0.51	0.28	-0.03	0.29	-0.07	0.99	1.00												
Pr	0.33	0.65	0.32	0.02	0.33	0.50	0.27	-0.07	0.24	-0.05	0.98	0.99	1.00											
Nd	0.38	0.65	0.33	0.06	0.33	0.51	0.27	-0.09	0.18	-0.03	0.95	0.97	0.99	1.00										
Sm	0.67	0.59	0.49	0.32	0.14	0.54	0.42	-0.08	0.19	0.09	0.79	0.82	0.88	0.92	1.00									
Eu	0.11	0.75	0.19	-0.12	0.64	0.48	0.13	-0.19	-0.24	-0.16	0.59	0.59	0.60	0.62	0.52	1.00								
Gd	0.84	0.52	0.60	0.52	-0.03	0.55	0.52	-0.06	0.19	0.18	0.57	0.61	0.68	0.74	0.95	0.39	1.00							
Tb	0.93	0.50	0.69	0.66	-0.13	0.61	0.63	-0.02	0.24	0.23	0.44	0.47	0.55	0.61	0.86	0.29	0.98	1.00						
Dy	0.97	0.51	0.75	0.75	-0.18	0.66	0.69	-0.01	0.25	0.26	0.37	0.40	0.47	0.53	0.80	0.24	0.93	0.99	1.00					
Ho	0.99	0.51	0.78	0.80	-0.21	0.70	0.74	0.00	0.27	0.28	0.33	0.35	0.42	0.48	0.74	0.21	0.89	0.96	0.99	1.00				
Er	0.99	0.52	0.82	0.85	-0.24	0.74	0.78	0.01	0.28	0.27	0.28	0.30	0.36	0.41	0.67	0.17	0.82	0.92	0.97	0.99	1.00			
Tm	0.97	0.50	0.84	0.88	-0.27	0.77	0.81	0.03	0.30	0.24	0.24	0.25	0.30	0.35	0.59	0.11	0.74	0.85	0.92	0.96	0.99	1.00		
Yb	0.93	0.49	0.84	0.88	-0.28	0.79	0.81	0.03	0.29	0.21	0.20	0.21	0.26	0.30	0.51	0.08	0.66	0.78	0.86	0.91	0.96	0.99	1.00	
Lu	0.92	0.49	0.83	0.87	-0.28	0.79	0.80	0.04	0.29	0.20	0.20	0.21	0.26	0.29	0.50	0.08	0.65	0.77	0.85	0.90	0.95	0.99	1.00	1.00

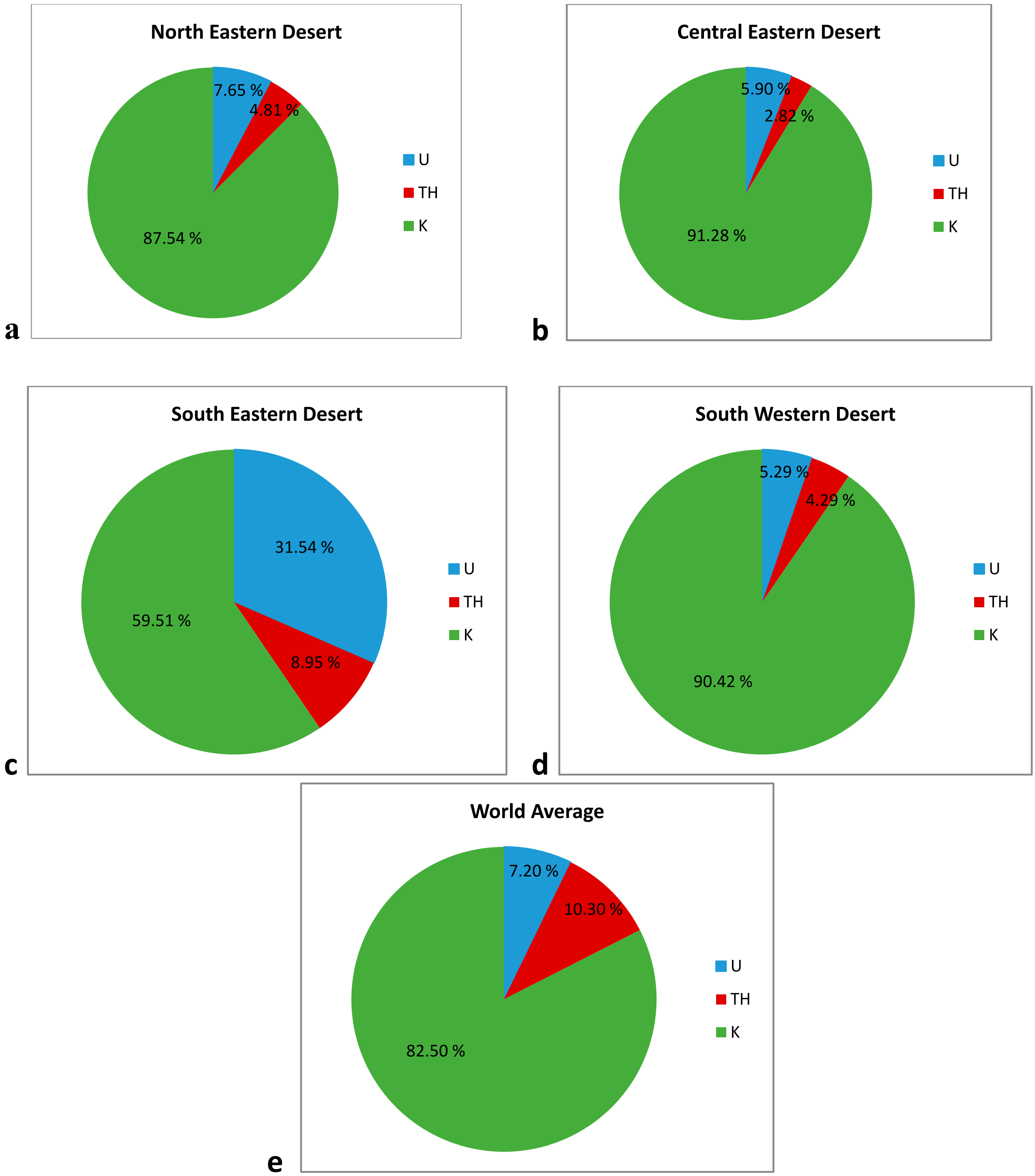

Fig. 6 **a–d** The average values for the relative contribution to ^{238}U, ^{232}Th and ^{40}K of the studied radioisotopes for the studied rocks of both Deserts compared to the World average

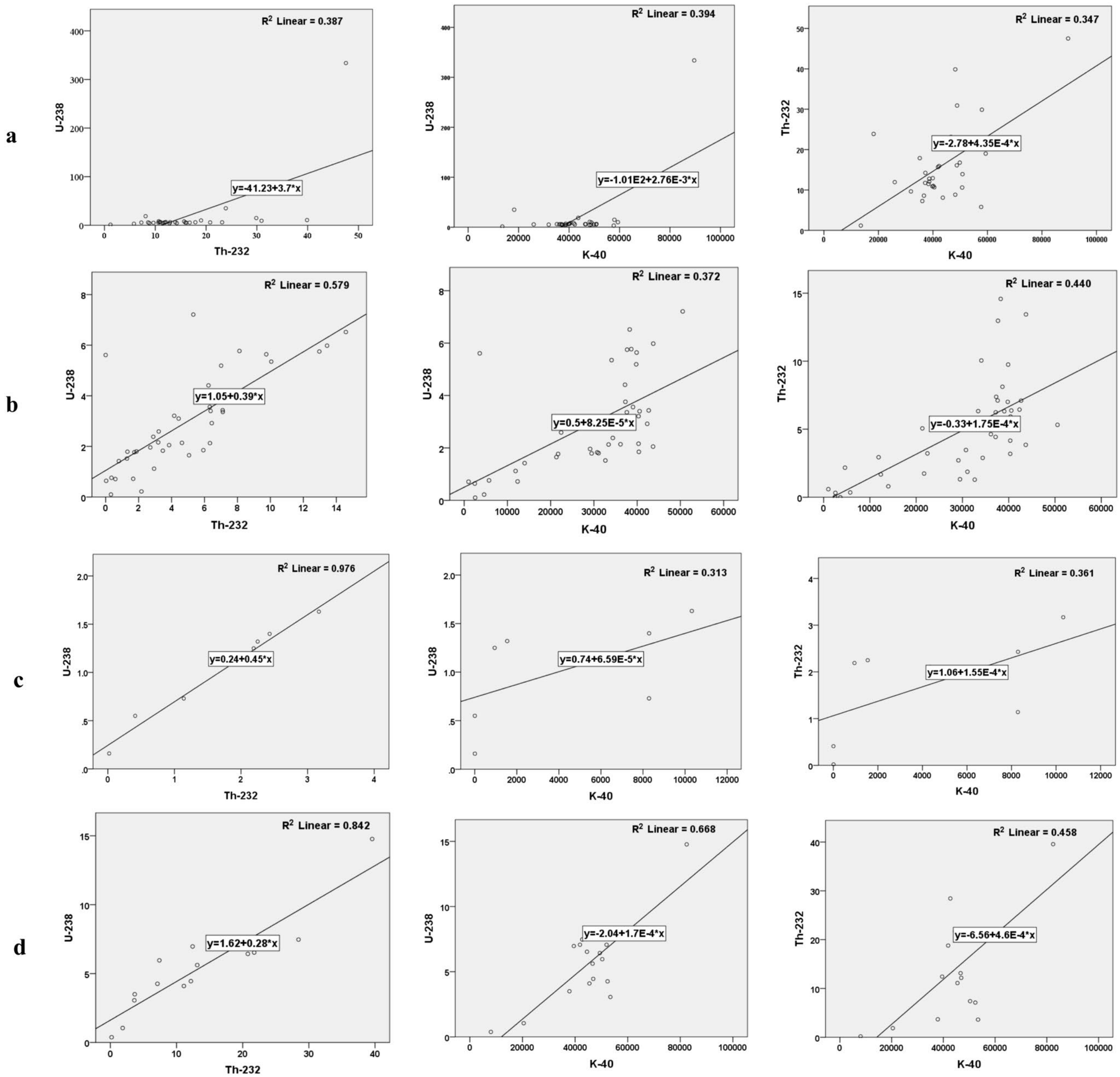

Fig. 7 Pearson correlation between the natural radionuclides (238U, 232Th and 40K) in the rock samples from NED, CED, SED and SWD

Acknowledgements The authors would like to express their great appreciation to the editors and the anonymous reviewers for their constructive comments to improve the manuscript.

Funding This research received no external funding.

Data availability All data analyzed during this study are included in this published article and its supplementary information files.

Declarations

Conflict of interest The authors declare that they have no competing interests.

References

Abbady AG (2004) Estimation of radiation hazard indices from sedimentary rocks in Upper Egypt. Appl Radiat Isot 60:111–114

Abd El-Fatah AA, Surour AA, Azer MK, Madani AA (2023) Integration of whole-rock geochemistry and mineral chemistry data for the petrogenesis of A-type ring complex from Gebel El Bakriyah Area Egypt. Minerals 13:1273. https://doi.org/10.3390/min13101273

Abdel-Gawad AE, Ali MA, Ghoneim MM, El-Taher A (2023) Natural radioactivity and mineral chemistry aspects of rare metal mineralization associated with mylonite at Wadi Sikait, South Eastern Desert Egypt. Int J Environ Anal Chem 103(10):2300–2317

Abdel-Meguid AA (1992) Late Proterozoic Pan African tectonic evolution of the Egyptian part of the Arabian-Nubian Shield. Middle East Research Center (MERC) Ain Shams Univ., Cairo Egypt. Earth Sci Ser 6:13–28

Abdel-Rahman AM, ElKibbi A (2001) Anorogenic magmatism: chemical evolution of the Mount El-Sibai A-type complex (Egypt), and implications for the origin of within-plate felsic magmas. Geol Mag 138(1):67–85

Abdul Adziz MI, Khoo KS (2018) An assessment of absorbed dose and radiation hazard index from soil around repository facility at Bukit Kledang, Perak, Malaysia. IOP Conf Ser: Mater Sci Eng 298:1–10

Abed NS, El-Feky MG, El-Taher A, Massoud EES, Khattab MR, Alqahtani MS, Hanfi MY (2022) Geochemical conditions and factors controlling the distribution of major, trace, and rare elements in sol Hamed granitic rocks, southeastern desert Egypt. Minerals 12(10):1245

Agbalagba EO, Osakwe ROA, Olarinoye IO (2014) Comparative assessment of natural radionuclide content of cement brands used within Nigeria and some countries in the world. J Geochem Explor 142:21–28

Akaad MK, Noweir A, Koth H (1979) Geology and petrography of the granite association of the Arabian Desert, orogenic belt of Egypt between lat. 25° 35′ and 26° 30′. Delta J Sci 3:107–151

Al-Zahrani BM, Alqannas HS, Hamidalddin SH (2020) Study and Simulation of the Natural Radioactivity (NORM) U-238, Th-232 and K-40 of igneous and sedimentary rocks of Al-Atawilah (Al-Baha) in Saudi Arabia. World J Nucl Sci Technol 10(4):171–181

Amin RM (2012) Gamma radiation measurements of naturally occurring radioactive samples from commercial Egyptian granites. Environ Earth Sci 67:771–775

Anjos R, Veiga R, Soare T, Santos A, Aguiar J, Frascá M (2005) Natural radionuclide distribution in Brazilian a commercial granites. Radiat Meas 39:245–253

Assran HM (2015) Petrology and radioactivity of the famous Aswan monumental red granites new occurrence, Gebel Um Shaghir area, South Western Desert Egypt. Arab J Geosci 8(9):1–11. https://doi.org/10.1007/s12517-014-1715-1

Awad HAM, Zakaly HMH, Nastavkin AV, El-Taher A (2022) Radiological implication of the granitoid rocks and their associated jasperoid veins, El-Missikat area, Central Eastern Desert Egypt. Int J Environ Anal Chem 102(19):8181–8194

Bashir M, Newman RT, Jones P (2019) Determination of activity concentration of 238U and 232Th series radionuclides in soil using a gamma-ray spectrometer in singles and coincidence modes. Appl Radiat Isotopes 154:108880

Bentor YK (1985) The crustal evolution of the Arabo-Nubian massif with special reference to the Sinai Peninsula. Precambrian Res 28:1–74

Beretka J& Matthew PJ, (1985) Natural radioactivity of Australian building materials, industrial wastes and by-products. J Health Phys 48(1):87–95

EC (European Commission) (1999) Radiological protection principles concerning the natural radioactivity of building materials. Directorate-General Environment, Nuclear Safety and Civil Protection, (Radiation Protection 112). Office for Official Publications of the EC

El-Gaby S, List FK, Tehrani R (1988) Geology, evolution and metallogenesis of the Pan-African belt in Egypt. In the Pan-African belt of Northeast Africa and adjacent areas: tectonic evolution and economic aspects of a late proterozoic Oregon. pp. 17–68

El-Gaby S, List FK, Tehrani R (1990) The basement complex of the Eastern Desert and Sinai. In: Said R (ed) The geology of Egypt. Balkema, Rotterdam, pp 175–184

El-Kammar AM, El-Hazik N, Mahdi M, Aly N (1997) Geochemistry of accessory minerals associated with radioactive mineralisation in the central Eastern Desert Egypt. J Afr Earth Sci 25(2):237–252

El Mezayen AM, Heikal MA, Abu Zeid IK, Omar SA, El-Feky MG, Lasheen ESR (2017) Petrography, geochemistry and radioactivity of El-Gidami granitic Rocks, Central Eastern Desert Egypt. Al-Azhar Bull Sci Conf 9:25–40

El-Taher A (2010) Gamma spectroscopic analysis and associated radiation hazards of building materials used in Egypt. Radiat Prot Dosim 138(2):166–173. https://doi.org/10.1093/rpd/ncp205

El-Taher A, Mohamed A, Yehia L, Salaheldin G, Elsman R, Khamis HA, Ahmed AA (2022) Spatial Distributions and Risk assessment of the natural radionuclides in the granitic rocks from Gabal Gattar II, Eastern Desert Egypt. Radiochemistry 64(6):783–792

Ergül HA, Murat Belivermis M, Önder Kılıç O, Topcuoglu S, Çotuk Y (2013) Natural and artificial radionuclide activity concentrations in surface sediments of Izmit Bay Turkey. J Environ Radioact 126:125–132

Fathallah O, Khattab MR (2023) Evaluation of environmental radioactivity and hazard impacts Saudi Arabia granitic rocks used as building materials. Minerals 13(2):165

Fowler AR, Ali KG, Omar SM, Eliwa HA (2006) The significance of gneissic rocks and synmagmatic extensional ductile shear zones of the Barud area for the tectonics of the North Eastern Desert Egypt. J Afr Earth Sci 46(3):201–220

Franz G, Puchelt H, Pasteels P (1987) Petrology, geochemistry and age relations of Triassic and tertiary volcanic rocks from SW Egypt and NW Sudan. J Afr Earth Sc 6(3):335–352

Frisch W, AbdelRahman AM (1999) Petrogenesis of the Wadi Dib alkaline ring complex, Eastern Desert of Egypt. Mineral Petrol 65(3):249–275

Gharib ME, Maurice AE, Ahmed AH, Asimow PD, Bakhit B& Selim HA, (2021) Evolution of a Neo-proterozoic island arc in the northern Arabian–Nubian Shield: volcanic rocks and their plutonic equivalents in the Hamash area, south Eastern Desert

Egypt. Precambrian Res 358:106145. https://doi.org/10.1016/j.precamres.2021.106145
Heikal MTS, Khedr M, Abd El Monsef M, Gomaa SR (2019) Petrogenesis and geodynamic evolution of Neoproterozoic Abu Dabbab Albite Granite, Central Eastern Desert of Egypt: petrological and geochemical constraints. J Afr Earth Sc 158:103518. https://doi.org/10.1016/j.jafrearsci.2019.103518
Hussein AA, Ali MM, El-Ramly MF (1982) A proposed new classification of the granites of Egypt. J Volcanol Geotherm Res 14:187–198
ICRP, International Commission on Radiological Protection (1991) Recommendations of the International Commission on Radiological Protection. ICRP Publication 60, Annals of the ICRP, Vol. 21, NI 1–3, Pergamon Press, Oxford
Kamar MS, Salem IA, El-Aassy IE, El-Sayed AA, Zakaly HM, Alzahrani AM, Lasheen ESR (2022) An investigation of high-level natural radioactivity and geochemistry of Neoproterozoic Dokhan volcanics: a case study of Wadi Gebeiy, Southwestern Sinai Egypt. Sustainability 14:9291. https://doi.org/10.3390/su14159291
Kitto ME, HainesK MTA (2009) Assessment of gamma-ray emissions from natural and manmade decorative stones. J Radioanal Nucl Chem 282:409
Klitzsch E, Schandelmeire H (1990) The geology of Egypt. In: Said R (ed) The geology of Egypt. A.A Balkema/Rotterdam/Brookfield
Knežević J, Kuzmanović P, Mrdja D, Todorović N, Bikit I, Hansman J (2020) Estimation of absorbed gamma dose rate from granite by Monte Carlo simulation approach. J Radiol Prot 40:596–611. https://doi.org/10.1088/1361-6498/ab8c22
Liégeois JP, Stern RJ (2010) Sr-Nd isotopes and geochemistry of granite-gneiss complexes from the Meatiq and Hafafit domes, Eastern Desert, Egypt: No evidence for pre-Neoproterozoic crust. J Afr EarthSci 57(1):31–40
Loizenbauer J, Wallbrecher E, Fritz H, Neumayr P, Khudeir AA, Kloetzli U (2001) Structural geology, single zircon ages and fluid inclusion studies of the Meatiq metamorphic core complex: Implications for Neoproterozoic tectonics in the Eastern Desert of Egypt. Precambrian Res 110(1):357–383
Maniar PD, Piccoli PM (1989) Tectonic discrimination of granitoids. Geol Soc Am Bull 101:635–643
Marocchi M, Righi S, Bargossi GM, Gasparotto G (2011) Natural radionuclides content and radiological hazard of commercial ornamental stones: an integrated radiometric and mineralogical-petrographic study. Radiat Meas 46:538–545
Merle L, Enn R (2012) Assessment of natural radiation exposure from building materials in Estonia. Proc Est Acad Sci 61(2):107–112
Middlemost EAK (1994) Naming materials in the magma/igneous rock system. Earth-Sci Rev 37:215–224. https://doi.org/10.1016/0012-8252(94)90029-9
Moghazi AM (2003) Geochemistry and petrogenesis of a High-K calc-alkaline Dokhan volcanic suite, South Safaga Area, Egypt: the role of late Neoproterozoic crustal extension. Precambr Res 125:161–178
O'Conner EA, Bennett JD, Rashwan AA, Nasr BB, Mansour MM, Romani RF, Sadek MF (1993) Crustal growth in the Nubian shield of South Eastern Desert, Egypt. In: Proc. Inter. Conf. 30 Years Cooper. pp 189–195
Orosun MM, Usikalu MR, Oyewumi KJ, Adagunodo TA (2019) Natural radionuclides and radiological risk assessment of granite mining field in Asa, North-central Nigeria. Methods X 6:2504–2514
Papadopoulos A, Altunkaynak Ş, Koroneos A, Ünal A, Kamaci Ö (2017) Geochemistry of uranium and thorium and natural radioactivity levels of the western Anatolian plutons, Turkey. Mineral Petrol 111:677–691
Pavlidou S, Koroneos A, Papastefanou C, Christofides G, Stoulos S, Vavelides M (2006) Natural radioactivity of granites used as building materials. J Environ Radioact 89:48–60
Pearce JA, Harris NB, Tindle AG (1984) Trace element discrimination diagrams for the tectonic interpretation of granitic rocks. J Petrol 25:956–983
Prasong K, Susaira A (2008) Natural radioactivity measurement in soil samples collected from the municipal area of Hat Yai District in Songkhla Province Thailand. KMITL Sci J 8(2):52–58
Qureshi AA, Tariq S, Shahid Manzoor KS, Calligaris C, Waheed A (2014) Evaluation of excessive lifetime cancer risk due to natural radioactivity in the rivers sediments of Northern Pakistan. J Radiat Res Appl Sciences 4(7):438–447
Ravisankar R, Vanasundari K, Suganya M, Raghu Y, Rajalakshmi A, Chandrasekaran A, Sivakunar S, Chandramohan J, Vijayagopal P, Venkatraman B (2014) Multivariate statistical analysis of radiological data of building materials used in Tiruvannamalai, Tamilnadu, India. Appl Radiat Isot 85:114–127
Ressetar R, Monrad J (1982) Chemical composition and tectonic setting of the Dokhan Volcanic Formation, Eastern Desert Egypt. J Afr Earth Sci 1(2):103–112. https://doi.org/10.1016/0899-5362(83)90002-7
Rickwood PC (1989) Boundary lines within petrologic diagrams which use oxides of major and minor elements. Lithos 22:247–263
Ries AC, Shackleton RM, Graham RH, Fitches WR (1983) Pan-African structures, ophiolites and mélange in the Eastern Desert of Egypt: a traverse at 26 N. J Geol Soc 140(1):75–95
Schandelmeier H, Darbyshire F (1984) Metamorphic and magmatic events in the Uweinat—Bir Safsaf Uplift (Western Desert/Egypt). Geol Rundsch 73(2):819–831
Sidique E, Elhaddad MA, Abdelwahab SF, El Hadek HH (2021) Health hazards assessment and geochemistry of ElSibai-Abu ElTiyur granites, Central Eastern Desert Egypt. Appl Sci 11:12002. https://doi.org/10.3390/app112412002
Sims PK, James HL (1984) Banded iron-formations of late Proterozoic age in the central Eastern Desert, Egypt; geology and tectonic setting. Econ Geol 79(8):1777–1784
Speer JA, Solberg TN, Becker SW (1981) Petrography of the uranium-bearing minerals of the Liberty Hill pluton, South Carolina: phase assemblages and migration of uranium in granitoid rocks. Econ Geol 76:2162–2175
Stern RJ (1981) Petrogenesis and tectonic setting of Late Precambrian ensimatic volcanic rocks, Central Eastern Desert of Egypt. Precambr Res 16(3):195–230
Stern RJ, Hedge CE (1985) Geochronologic and isotopic constraints on late Precambrian crustal evolution in the Eastern Desert of Egypt. Am J Sci 285(2):97–127
Stockdale A, Bryan ND (2013) The influence of natural organic matter on radionuclide mobility under conditions relevant to cementitious disposal of radioactive wastes: a review of direct evidence. Earth Sci Rev 121:1–17. https://doi.org/10.1016/j.earscirev.2013.02.007
Taalab SA, Al Meshari M, Alzamil Y, Ahmad A, Amjad RA, Waheed HM, El-Taher A (2023) Radiological and ecological hazards evaluation of episyenite used as building materials. J Radioanal Nucl Chem 332(4):2057–2075
Tzortzis M, Tsertos H, Christofides S, Christodoulides G (2003) Gamma radiation measurements and dose rates in commercially used natural tiling rocks (granites). J Environ Radioact 70:223–235
UNSCEAR (2000) Sources and effects of ionizing radiation: United Nations Scientific Committee on the Effects of Atomic Radiation. Report to the General Assembly, with Scientific Annexes. United Nations
UNSCEAR (2008) Report: sources and effects of ionizing radiation. The United Nations Scientific Committee on the Effects of Atomic Radiation: New York, NY, USA, 2010
Uosif MAM, El-Taher A (2008) Radiological assessment of Abu-Tartur phosphate, Western Desert Egypt. J Radiat Protect Dosim 130(2):228–235

Viruthagiri G, Ponnarasi K (2011) Measurement of natural radioactivity in brick samples. Adv Appl Sci Res 2(2):103–108

Wang Y, Lesher M, Lightfoot P, Pattison E, Golightly J (2020) Geochemistry and petrogenesis of mafic and ultramafic inclusions in Sublayer and Offset Dikes Sudbury Igneous Complex Canada. J Petrol. https://doi.org/10.1093/petrology/egaa059

Whalen JB, Currie KL, Chappell BW (1987) A-type granites: geochemical characteristics, discrimination and petrogenesis. Contrib Mineral Petrol 95:407–419. https://doi.org/10.1007/BF00402202

Windley BF (1977) The evolving continents. J. W. Arrow Smith Ltd, Bristol, p 385

Xinwei W, Lingqing XJ (2006) Radiometric analysis of Chinese commercial granites. J Radioanal Nucl Chem 267:669–673

Zalewski M, Tomczak M, Kapata J (2001) Radioactivity of building materials available in Northeastern Poland. Pol J Environ Stud 10(3):183–188